AD-A058 816 SOUTHWEST RESEARCH INST SAN ANTONIO TEX F/G 19/4
DEVELOPMENT OF A BLAST SIMULATOR FOR TESTING SIMULATED AIRCRAFT--ETC(U)
JUL 78 E D ESPARZA, A B WENZEL DAAD05-76-C-0726
UNCLASSIFIED SWRI-02-4374 JTCG/AS-76-T-004 NL

| OF |
AD
A058816

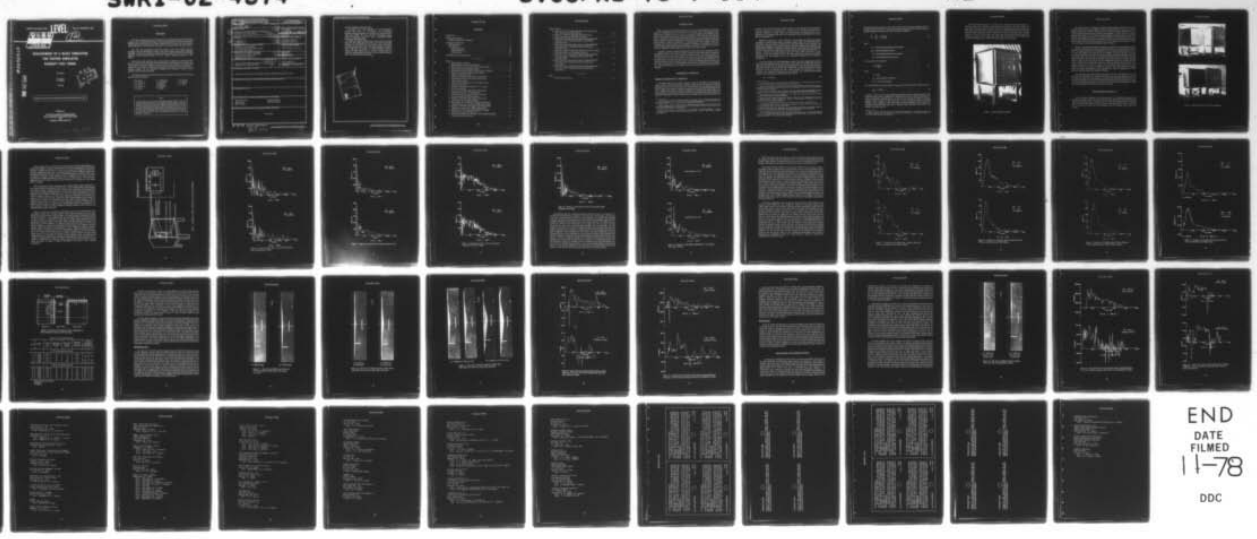

END
DATE
FILMED
11-78
DDC

REPORT JTCG/AS-76-T-004

LEVEL II

FIELD OF INTEREST: 03.01

12 B.S.

JTCG/AS

AD A058816

DDC FILE COPY

DEVELOPMENT OF A BLAST SIMULATOR FOR TESTING SIMULATED AIRCRAFT FUEL TANKS

Final Report

E. D. Esparza
A. B. Wenzel

July 1978

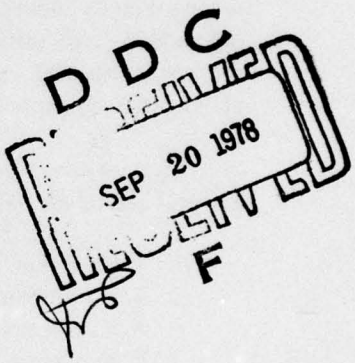

Prepared for

THE JOINT LOGISTICS COMMANDERS
JOINT TECHNICAL COORDINATING GROUP
ON
AIRCRAFT SURVIVABILITY

FOREWORD

This report summarizes results of tests performed by Southwest Research Institute, San Antonio, TX for the Survivability Branch, Air Force Flight Dynamics Laboratory (AFFDL), Wright-Patterson AFB, OH, under contract DAAD05-76-C-0726. The work was performed between September 1975 and December 1976, and C. Anderson (AFFDL) was project engineer.

The work was sponsored by JTCG/AS as part of the 3-year TEAS (Test and Evaluation, Aircraft Survivability) program. The TEAS program was funded by DDR&E/ ODDT&E. The effort was conducted under the direction of the JTCG/AS Technology R&D Subgroup under JTCG/AS Project TF-6-14-F, *Missile Warhead Simulation - Blast Effects.*

Anti-aircraft missile warheads pose a severe threat to aircraft even when the missile misses the aircraft. The threat from missile warheads can be divided into two primary areas for proximity detonation, fragments and blast. This report describes the development, calibration, and testing of a blast simulator capable of varying the blast parameters (i.e., pressure, impulse, and time duration), simulating those obtained at various standoff distances from prototype detonation.

The authors would like to acknowledge the contributions of the government technical monitor and their colleagues:

W. E. Baker
R. A. Cervantes
A. C. Garcia
E. R. Garcia, Jr.
L. R. Garza
V. J. Hernandez
J. C. Hokanson
J. Hollifield
L. D. Martinez
S. K. Miller
P. K. Moseley
C. A. Pierson
F. E. Slater

NOTE

A technical report was prepared by the Vulnerability Assessment Subgroup of the Joint Technical Coordinating Group on Aircraft Survivability in the Joint Logistics Commanders' organization. Because the Services' aircraft survivability development programs are dynamic and changing, this report represents the best data available to the subgroup at this time. It has been coordinated and approved at the JTCG subgroup level. The purpose of the report is to exchange data on all aircraft survivability programs, thereby promoting interservice awareness of the DOD aircraft survivability program under the cognizance of the Joint Logistics Commanders. By careful analysis of the data in this report, personnel with expertise in the aircraft survivability area should be better able to determine technical voids and areas of potential duplication or proliferation.

SECURITY CLASSIFICATION OF THIS PAGE (When Data Entered)

REPORT DOCUMENTATION PAGE

READ INSTRUCTIONS BEFORE COMPLETING FORM

1. REPORT NUMBER: JTCG/AS-76-T-004	2. GOVT ACCESSION NO.
3. RECIPIENT'S CATALOG NUMBER	
4. TITLE (and Subtitle): Development of a Blast Simulator for Testing Simulated Aircraft Fuel Tanks,	5. TYPE OF REPORT & PERIOD COVERED: Final report, September 1975 - December 1976
6. PERFORMING ORG. REPORT NUMBER: SWRI - 02-4374	
7. AUTHOR(s): E. D. Esparza, A. B. Wenzel	8. CONTRACT OR GRANT NUMBER(s): DAAD05-76-C-0726
9. PERFORMING ORGANIZATION NAME AND ADDRESS: Southwest Research Institute, 6220 Culebra Road, P.O. Drawer 28510, San Antonio, TX 78284	10. PROGRAM ELEMENT, PROJECT, TASK AREA & WORK UNIT NUMBERS: JTCG/AS Project TF-6-14-F
11. CONTROLLING OFFICE NAME AND ADDRESS: JTCG/AS Central Office, AIR-5204J, Naval Air Systems Command, Washington, DC 20361	12. REPORT DATE: July 1978
	13. NUMBER OF PAGES: 42
14. MONITORING AGENCY NAME & ADDRESS (if different from Controlling Office): Air Force Flight Dynamics Laboratory, Wright-Patterson AFB, OH 45433	15. SECURITY CLASS. (of this report): UNCLASSIFIED
	15a. DECLASSIFICATION/DOWNGRADING SCHEDULE

16. DISTRIBUTION STATEMENT (of this Report)

Approved for public release; distribution unlimited. Statement applied July 1978.

17. DISTRIBUTION STATEMENT (of the abstract entered in Block 20, if different from Report)

18. SUPPLEMENTARY NOTES

19. KEY WORDS (Continue on reverse side if necessary and identify by block number)

Aircraft fuel tank
Blast loading
Blast simulator
Dynamic response
Structural damage

20. ABSTRACT (Continue on reverse side if necessary and identify by block number)

See reverse.

DD FORM 1 JAN 73 1473 EDITION OF 1 NOV 65 IS OBSOLETE
S/N 0102-014-6601

328 200

SECURITY CLASSIFICATION OF THIS PAGE (When Data Entered)

Air Force Flight Dynamics Laboratory

Development of a Blast Simulator for Testing Simulated Aircraft Fuel Tanks, by E. D. Esparza and A. B. Wenzel, Southwest Research Institute, San Antonio, TX. Wright-Patterson AFB, OH, AFFDL, for Joint Technical Coordinating Group/ Aircraft Survivability, July 1978. 42 pp. (JTCG/AS-76-T-004, publication UNCLASSIFIED.)

Anti-aircraft missile warheads pose a severe threat to aircraft even when the missile misses the aircraft. The threat from missile warheads can be divided into two primary areas for proximity detonation, fragments and blast. This report describes the development, calibration, and testing of a blast simulator capable of varying the blast parameters (i.e., pressure, impulse, and time duration), simulating those obtained at various standoff distances from a prototype warhead detonation.

CONTENTS

Figures:

Figures (Contd.):

Table:

INTRODUCTION

When an anti-aircraft missile warhead does not hit an aircraft directly but detonates nearby, the missile still poses a severe threat to the intended target. Critical damage to the aircraft can be inflicted to the fuel tanks by high speed fragments, hot fragments, blast pressure, and the high temperature environment produced by the detonation. Experimental tests are essential to assess the fuel tanks vulnerability to such threats; however, full scale tests are expensive and time consuming. Therefore, the capability to simulate the significant threat aspects to perform evaluations in a controlled and realistic manner need to be developed. This report describes the development, calibration, and testing of a chamber system which simulates the blast pressure loading on simulated fuel tanks as they may occur from the explosion of missile warheads in the vicinity of combat aircraft.

Generally, to assess the damage contribution of blast as part of the total threat effect is very difficult. This is true for actual combat incidents and arena tests where the warhead is detonated statically in the vicinity of aircraft tankage. Therefore, the primary objective of the program was to develop test techniques that provide the capability of applying realistic pressures with the proper time profile to the walls of typical fuel tank structures. The second objective was to test aluminum plates and assess the damage effects that result from this type of blast loading. The investigation focused on the most likely types of response (i.e., structural damage and fuel leakage) and the blast parameters that may affect this response.

EXPERIMENTAL APPROACH

DESIGN OF EXPERIMENTAL APPARATUS

The blast loading on an aircraft caused by a near miss detonation of an anti-aircraft missile warhead was simulated using a partially vented box structure which had internal dimensions of 3 by 3 by 3 feet (0.91 by 0.91 by 0.91 meters) with one open side for placing the test plates. This chamber is similar to suppressive structures analysed and designed[1] for use in reducing the hazards of accidental explosions in facilities that contain and process high explosives. Scaled models of these uniformly vented multi-layered structures have been tested[2,3] to determine the blast attenuation to the outside of the structure and measure the

---

[1] Edgewood Arsenal. *Analysis and Preliminary Design of a Suppressive Structure for a Melt Loading Operation*, by W. E. Baker, P. A. Westine, P. A. Cox, and E. D. Esparza, Southwest Research Institute. San Antonio, Texas. May 1976. 102 pp. (EM-CR-76056, Contract No. DAAD05-74-C-0751, publication UNCLASSIFIED.)

[2] Ballistic Research Laboratories. *Blast Attenuation Outside Cubical Enclosures Made Up of Selected Suppressive Structure Panel Configurations*, by R. N. Schumacher and W. O. Ewing. Aberdeen Proving Ground, MD, BRL, September 1975. (BRL MR 2537, publication UNCLASSIFIED.)

[3] Ballistic Research Laboratories. *Internal Pressure From Explosions in Suppressive Structures*, by C. Kingery, R. Schumacher, and W Ewing. Aberdeen Proving Ground, MD, BRL, June 1975. (BRL IMR 403, publication UNCLASSIFIED.)

pressures on the walls from internal explosions. Other experimental and analytical programs have been conducted to characterize the internal and external blast environment from confined explosions in cubicles; which are vented through one opening on one side as opposed to the uniform venting used in the suppressive structures through five of the six sides of the enclosure[4-10].

Whether the structure is vented uniformly or only through one opening, an internal detonation of a high-explosive causes a two-phase pressure history. The first consists of the initial blast wave and subsequent reflections from the inner surfaces of the enclosure. This initial shock impinging on the structure applies an intense loading of short duration. This loading, which consists of a reflected pressure and impulse, can be estimated with reasonable accuracy from test data of blast waves normally reflected from rigid, plane surfaces[11-13]. However, reflections and reinforcements can occur in the corners and edges of a cubic structure so that the implosion process after shock reflection is complex and irregular. Fortunately, the latter shocks seem to be attenuated compared to the initial one (footnote 3).

The second phase of the internal loading consists of the lower amplitude gas pressure which decays considerably slower, depending on the amount of venting, than the initial blast wave. Because the two phases are not separated in time, the peak gas pressure is difficult to measure directly and thus only estimates can be made from experimental data. To better use the gas pressure data from vented structure tests (footnote 1), a model analysis of the explosion venting process was conducted. The resulting nondimensional scaling law was subsequently modified (footnotes 8 and 9).

$$\bar{P} = f_1(\bar{\tau}, \bar{P}_1, \gamma) \qquad (1)$$

---

[4] J. F. Procter and W. S. Filler. "A Computerized Technique for Blast Loads From Confined Explosions," presented at the 14th Annual Explosives Safety Seminar, New Orleans, LA, November 1972.

[5] Naval Construction Battalion Center. *Blast Environment From Fully and Partially Vented Explosions in Cubicles*, by W. A. Keenan and J. E. Tancreto, Civil Engineering Laboratory, Port Hueneme, CA, November 1975. (Technical Report R828, publication UNCLASSIFIED.)

[6] Joint Technical Coordinating Group for Munitions Effectiveness. *Internal Blast Damage Mechanisms Computer Program*, by J. F. Proctor, Tinker AFB, OK, JTCG/ME, April 1973. (JTCG/ME-73-3, publication UNCLASSIFIED.)

[7] Naval Weapons Center. *Venting of Explosions*, by G. F. Kinney and R. G. S. Sewell. China Lake, CA, NWC, July 1974. (NWC TM 2448, publication UNCLASSIFIED.)

[8] Edgewood Arsenal. *Estimates of Blowdown of Quasi-Static Pressures in Vented Chambers*, by W. E. Baker and G. A. Oldham, Southwest Research Institute, San Antonio, TX, November 1975. (EM-CR-76029, Contract No. DAAA15-75-C-0083, publication UNCLASSIFIED.)

[9] J. A. Owczarek. *Fundamentals of Gas Dynamics*. International Textbook Company, Scranton, PA, 1964.

[10] H. R. W. Weibull. "Pressures Recorded in Partially Closed Chambers at Explosion of INT Charges", *Annals of the New York Academy of Sciences*, 152, Art. 1, October 1968.

[11] Ballistic Research Laboratories. *Measurements of Normally Reflected Shock Waves From Explosive Charges*, by W. H. Jack, Jr. Aberdeen Proving Ground, MD, BRL, 1968. (BRL MR 1499, publication UNCLASSIFIED.)

[12] W. E. Baker. *Explosions in Air*. University of Texas Press, Austin, TX, 1973.

[13] U.S. Army MERDC. *Measurements of Pressures and Impulses at Close Distances From Explosive Charges Buried and in Air*, by A. B. Wenzel and F. D. Esparza, Southwest Research Institute, San Antonio, TX, August 1972. (02-3132, Contract No. DAAK 02-71-C-0393, publication UNCLASSIFIED.)

where $\bar{P}$ is the scaled pressure at some scaled time $\bar{\tau}$ and $\bar{\gamma}$ is the ratio of specific heats for the gas within the structure. $\bar{P}_1$ is the peak scaled gas pressure which for structures with no or small venting can be shown to be related to another scaling term

$$\bar{P}_1 = \frac{P_1}{p_o} = f_2\left(\frac{E}{p_o V}\right) \tag{2}$$

where

P_1 = maximum (initial absolute gas pressure)

p_o = local atmospheric pressure

E = total energy released by the explosion

V = internal volume of the structure.

The scaled time $\bar{\tau}$ is defined as

$$\bar{\tau} = \frac{t a_o A_v}{V} \tag{3}$$

where

t = time

a_o = sound velocity of outside air

A_v = vent area of structure

The scaled duration of the gas pressure is $\bar{\tau}_{max}$ and is a unique function of $\bar{P}_1$ (footnote 8)

$$\bar{\tau}_{max} = f_3(\bar{P}_1) \tag{4}$$

Equations 2 and 4 can be used to plot experimental data and compare that data with theoretical and analytical predictions[14]. These plots can then be used for estimating the amount of explosive, internal volume, and the vent area required to produce a given gas pressure history. Because of the large scatter in the experimental data for plotting Equation 4, the rearranged equation by Kinney and Sewell (footnotes 7 and 8) which fits through the data fairly well, was used to obtain the initial estimates of the duration and impulse in the blast chamber.

---

[14] Edgewood Arsenal. *Blast Pressures Inside and Outside Suppressive Structures*, by E. D. Esparza, W. E. Baker, and G. A. Oldham, Southwest Research Institute. San Antonio, TX, December 1975. (EM-CR-76042. Contract No. DAAA15-75-C-0083, publication UNCLASSIFIED.)

The blast simulator designed and built for this program (as shown in Figure 1) is similar in design to the uniformly vented suppressive structures. The five sides consist of an inner layer of structural angles uniformly spaced and a perforated plate as the outer layer. This double layer design was chosen over a single vented plate primarily because test data from the similar suppressive structures showed that a closed, evenly spaced layer of angles seemed to break the initial shock wave better than flat surfaces and thus reduced the number and intensity of the subsequent reflections. (See footnotes 2 and 3.) This would then make it slightly easier to tailor the pressure profile on the test plate.

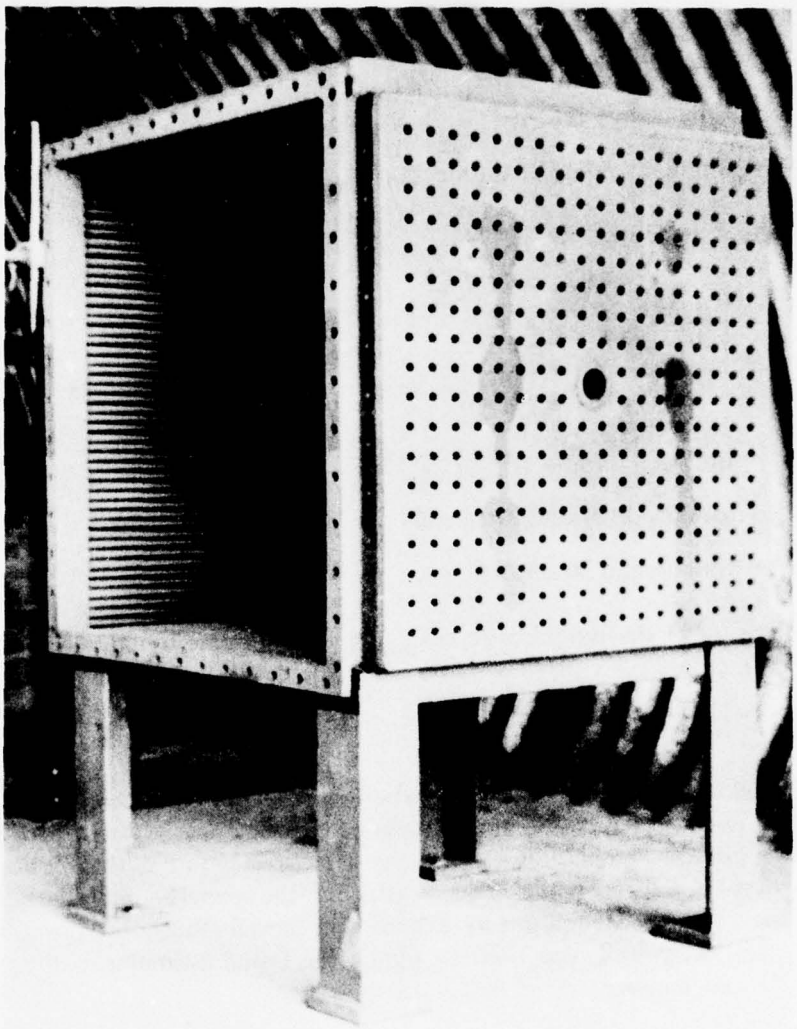

Figure 1. Blast Simulation Chamber.

The initial amount of venting was estimated using Equation 4 so that the shortest duration desired in the testing program could be obtained. This vent area was then evenly distributed among the five sides. All sides except the back are the same. Because one of the chamber design requirements was to provide the capability, in future work, for launching fragments through the box for tests combining fragment and blast effects, the back was designed with a large circular hole. The venting provided by this hole was accounted for in trying to make the blast chamber vent uniformly; also provisions were incorporated to allow closing some of the vent area in each side by the use of external plates covering a certain area so the longer loading durations required could be obtained.

However, once testing was begun to calibrate and develop the proper pressure history, the amount of venting required was considerably more than had been provided on the blast tank. The easiest and best way to increase the vent area was to enlarge the circular hole on the back side opposite the open face of the chamber. This was not only a less time consuming operation but also made the future shooting of fragments through the chamber much easier. Since the back side now provided the majority of the vent area, the longer loading durations were achieved by partially closing this circular area, an easier task than closing an area on all five vented sides. This modified design made the chamber resemble more a cubicle vented through one side than a uniformly vented structure. However, the venting provided by all the sides along with the internal angles decreased the shock reflections within the chamber as opposed to solid flat walls. The angles and perforated plates were sized conservatively so the repeated loads expected throughout the testing program would not appreciably damage the chamber.

The open side of the blast chamber was designed so that it could be mated to a cubic tank which has provisions for accepting replaceable front and back aluminum walls. The simulated fuel tank frame was designed to sustain repeated blast loads without damage even though the aluminum test plates were sometimes damaged during the tests. Figure 2 shows the simulated fuel tank and how it mates with the blast chamber. The two open sides hold the aluminum plates which simulate aircraft fuel tank walls.

TEST PROGRAM AND RESULTS

The two primary objectives of this program were to: (1) develop test techniques for simulating the blast loads on fuel tanks from near-miss, anti-aircraft warhead detonations, and (2) test aluminum panels simulating fuel tank walls and determine the level of damage from the blast loading. A total of 78 experiments were conducted. Of these, 52 tests were fired to develop a method for load simulation using the partially vented cubic blast chamber.

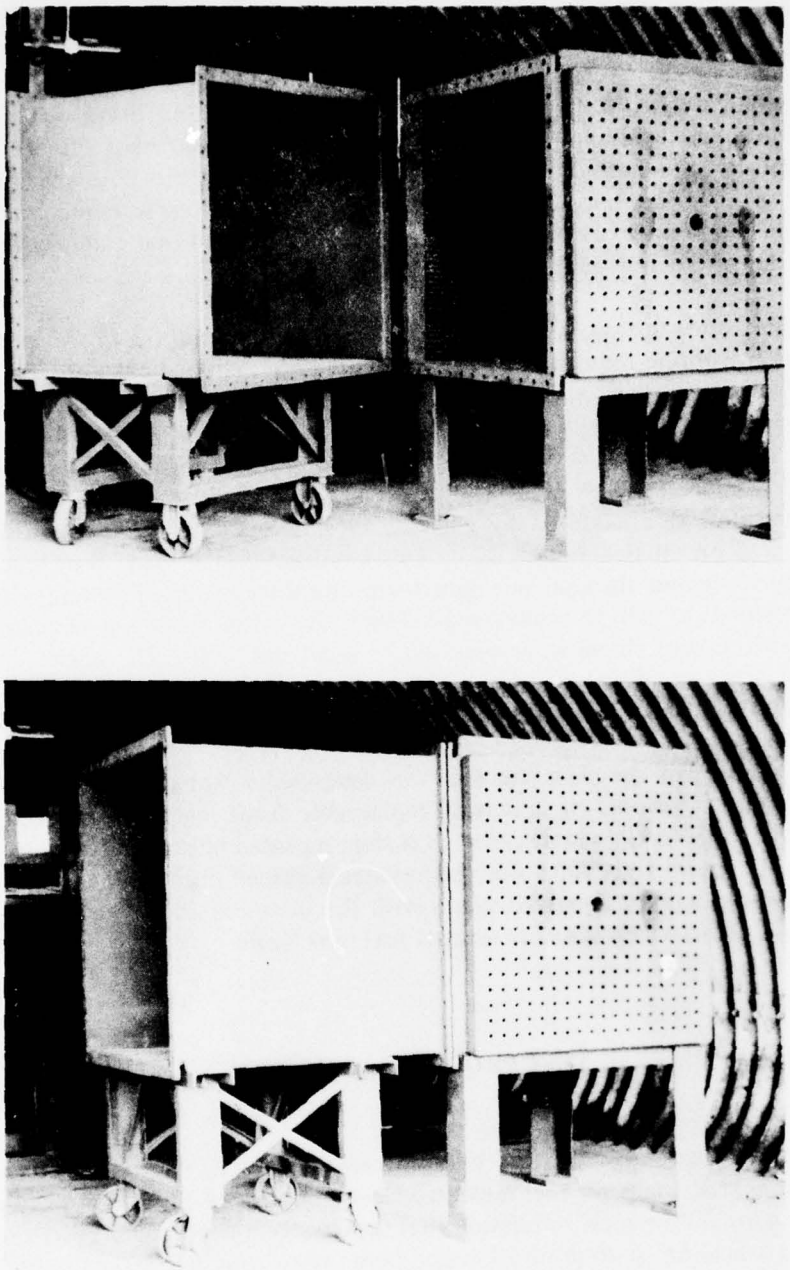

Figure 2. Blast Chamber and Fuel Tank Simulators.

The results of some of the tests to develop the blast loading simulation technique were of the go/no go type until a suitable scheme was found for obtaining the desired loading profile. Consequently, the number of usable calibration points for the blast tank is smaller than the number of tests fired. The tests on the aluminum plates yielded results which ranged from no damage to severe deformation so again the number of measurable deformations is less than the number of experiments using the aluminum panels.

CALIBRATION TESTS

As discussed in *Experimental Approach*, the primary objective was to develop a blast simulation technique using a vented box structure able to simulate reflected blast overpressures ranging from 10 to 50 psig (69 to 345 kPa) with a corresponding impulse range of approximately 60 to 150 psi • msec (414 to 1034 kPa • msec). By detonating a high-explosive within a partially vented chamber, a two phase loading develops within the structure. The problem then was how to attenuate and reshape the initial shock blast and its reflections so as to obtain a repeatable peak pressure for a given charge weight and the proper decay time of the gas pressure to develop the corresponding impulse wanted. From Equation 2, we know that the peak gas pressure in a partially vented structure is strictly a function of the energy released and the size of the internal volume. Therefore, the mass of the explosive used controls the peak gas pressure in a constant volume structure. The reflected peak pressure produced by a high-explosive detonation depends on the scaled distance (actual distance between the charge and the measurement point) and the charge weight. At close scaled distances the overpressure also depends on the geometry of the charge. The estimated charge size and the distance between the charge and the test plates within the blast chamber were such that the geometry was expected to be a significant influence on the amplitude of the initial reflected shock pressure. Therefore, 26 tests were conducted to determine the effects of charge geometry on the reflected peak pressure at the test plate from several different charge sizes.

To do this, a 1-inch (25.4-mm) steel plate was used on the open-side of the blast chamber as shown in Figure 3. This plate had two pressure transducer locations, one at the center and the other offset about 6 inches (152.4 mm) horizontally. The transducers used were one Susquehanna Model ST-2 with a pressure range of 0.1 to 500 psi (0.7 to 3448 kPa) and one Kulite Model HKS-275-1000 with a pressure range of 0 to 1000 psi (0 to 6895 kPa). The ST-2 piezoelectric transducer was connected to a source follower/amplifier unit for impedance matching and amplification. The piezoresistive Kulite transducer was connected to a strain gage signal conditioner/amplifier for power, balance, and amplification. The signals from both units were recorded on a Bell & Howell Model CPR 4010 FM, Wideband Group I magnetic tape recorder at a recording speed of 30 in/sec. The data were then played back at 1 7/8 in/sec through a Bell & Howell Type 1-026 galvanometer preamplifier into a Bell & Howell Type 5-134 oscillograph recorder with 1500 Hz galvanometers. This electronic equipment is shown in Figure 4. The oscillograph records were then processed using a Hewlett-Packard Model 9830A calculator with a 9864A digitizer and 9862A plotter to obtain permanent copies of the data with engineering units for analysis.

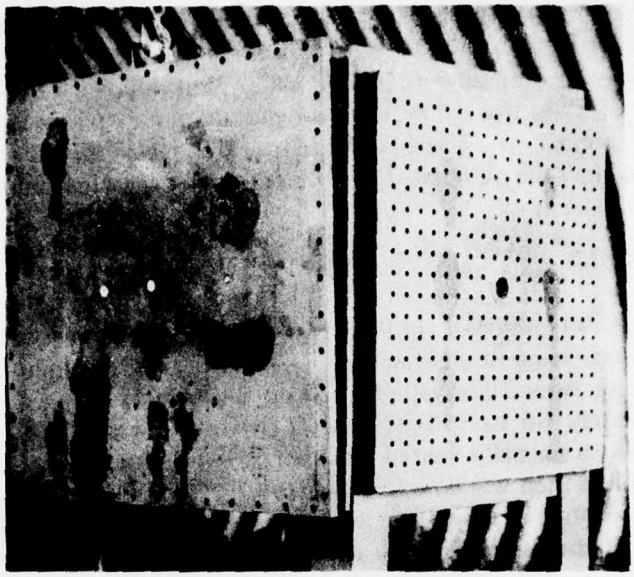

Figure 3. Blast Chamber with 1-Inch (25.4-mm) Steel Test Plate.

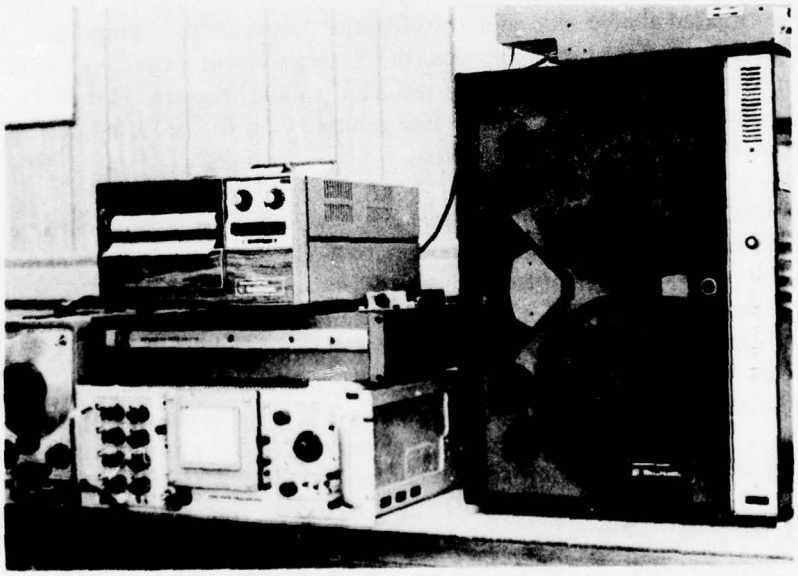

Figure 4. Pressure Record and Play-Back System.

The first group of the 26 calibration experiments were conducted using Detasheet L, a commercial explosive containing approximately 80% PETN (pentaerythritol tetranitrate) explosive by weight with inert binder material used to produce this explosive in sheet form. Since the internal peak gas pressure is a function of the explosive weight, the quantities of explosive presented are always the amount of PETN present in a given charge. Thus, a mass of explosive of 40 gm actually required 50 gm of Detasheet L to be used. The sheet explosive was configured into sheets as large as 6.5 by 6.5 inches (165 by 165 mm) and into small cubes 1 inch (25.4 mm) to the side. Several different size charges were used ranging from 17 to 88 gm.

The second group of these experiments used similar geometry charges of Detasheet C. The C-type contains less primary explosive (71%), so that a slightly larger charge mass had to be used to obtain an equivalent mass of PETN as the L-type sheet. These experiments showed that by using a relatively thin sheet of about 20 to 40 in^2 (129 to 258 cm^2) with a thickness of about 0.042 to 0.084 inch (1.1 to 2.2 mm) oriented perpendicular to the test plate as shown in Figure 5, one could obtain significant reductions on the initial shock pressure versus the other extreme, a similar size sheet oriented parallel to the test plate. In both cases, the charge was suspended using nylon string loop and keeping it as flat as possible; pieces of tape were used to keep the charge from rotating once suspended. The DuPont E-106 detonator was placed on the explosive sheet using a much smaller piece of sheet explosive to hold it in place. (Detasheet explosive sticks very well to itself so the detonator stayed in place quite well.)

Figure 6 shows the two pressure measurements made on the instrumented 1-inch (25.4-mm) steel plate for a 36.5-gm explosive sheet oriented normally to the test plate. Similar measurements from a 38-gm explosive cube which produced a higher peak pressure are shown in Figure 7. These pressures also are much higher than the expected peak gas pressure of about 25 to 30 psig (173 to 207 kPa) for this size charge. Measurement of the gas pressure is difficult because of the large number of reflections plus the very high initial shock pressure present. However, by using an acoustic filter (footnote 3) in front of the pressure transducer, a measure of the gas pressure and its decay can be obtained as shown in Figure 8. These gas pressures were generated by 37 gm charges and measured through a special transducer holder on the side of the blast chamber. Figure 9 shows the pressure at the center of the test plate from a sheet of explosive perpendicular to the plate with a charge mass of 81.5 gm. From these types of data, it became obvious that even though charge geometry was important in reducing the initial shock pressure, an attenuator was necessary to obtain further pressure reduction and smoothing out of the reflections. Thus, a number of experiments were conducted using a variety of neoprene foam rubber, open and closed and open cell foam, in different thicknesses in an effort to find a suitable combination.

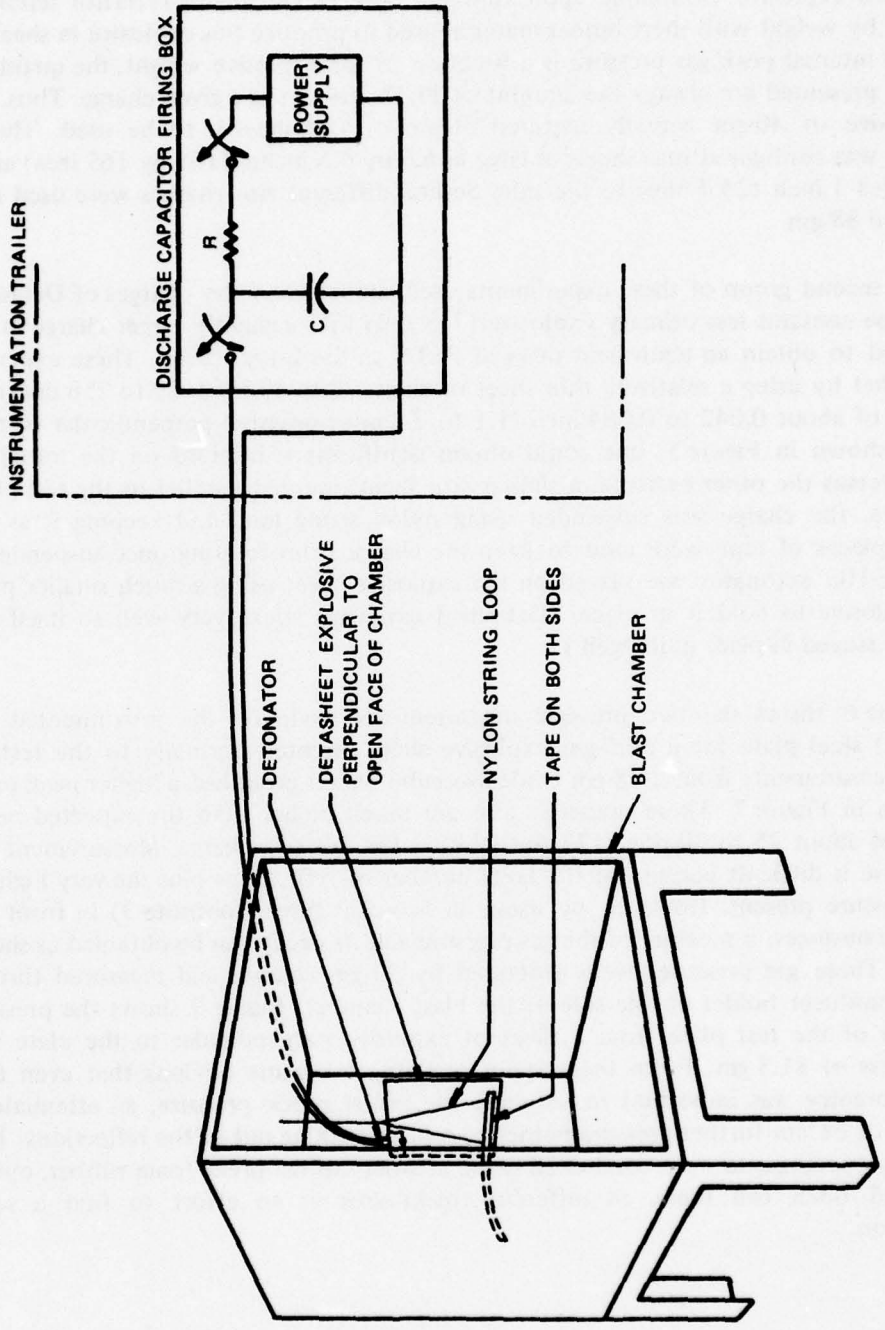

Figure 5. Installation of Sheet Explosive and Firing Circuit Diagram.

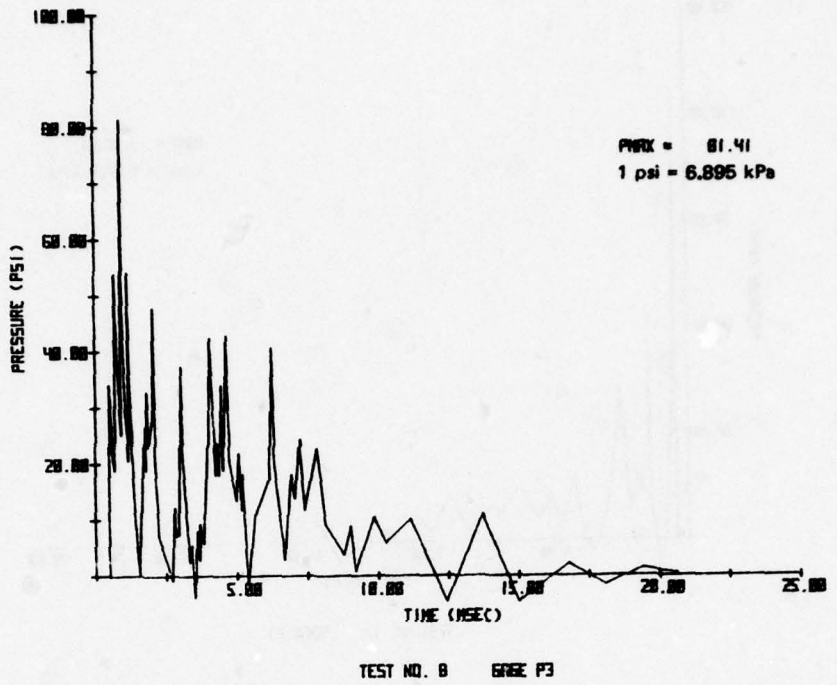

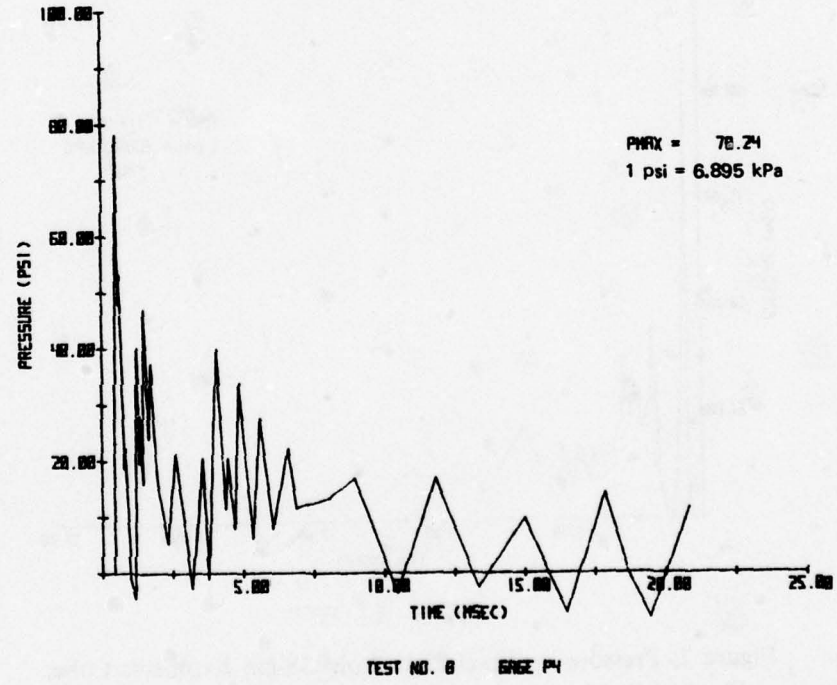

Figure 6. Pressure on Steel Plate from 36.5-gm Explosive Sheet Perpendicular to Plate.

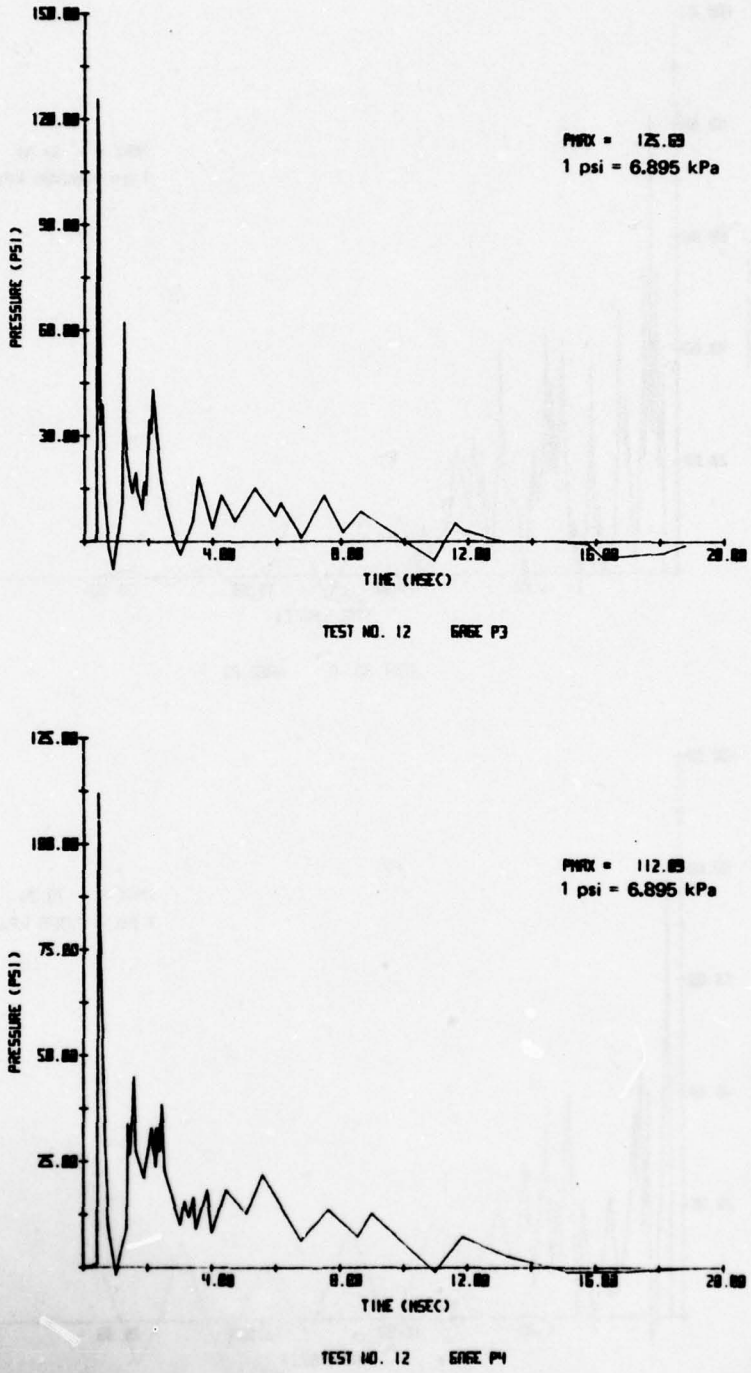

Figure 7. Pressure on Steel Plate from 38-gm Explosive Cube.

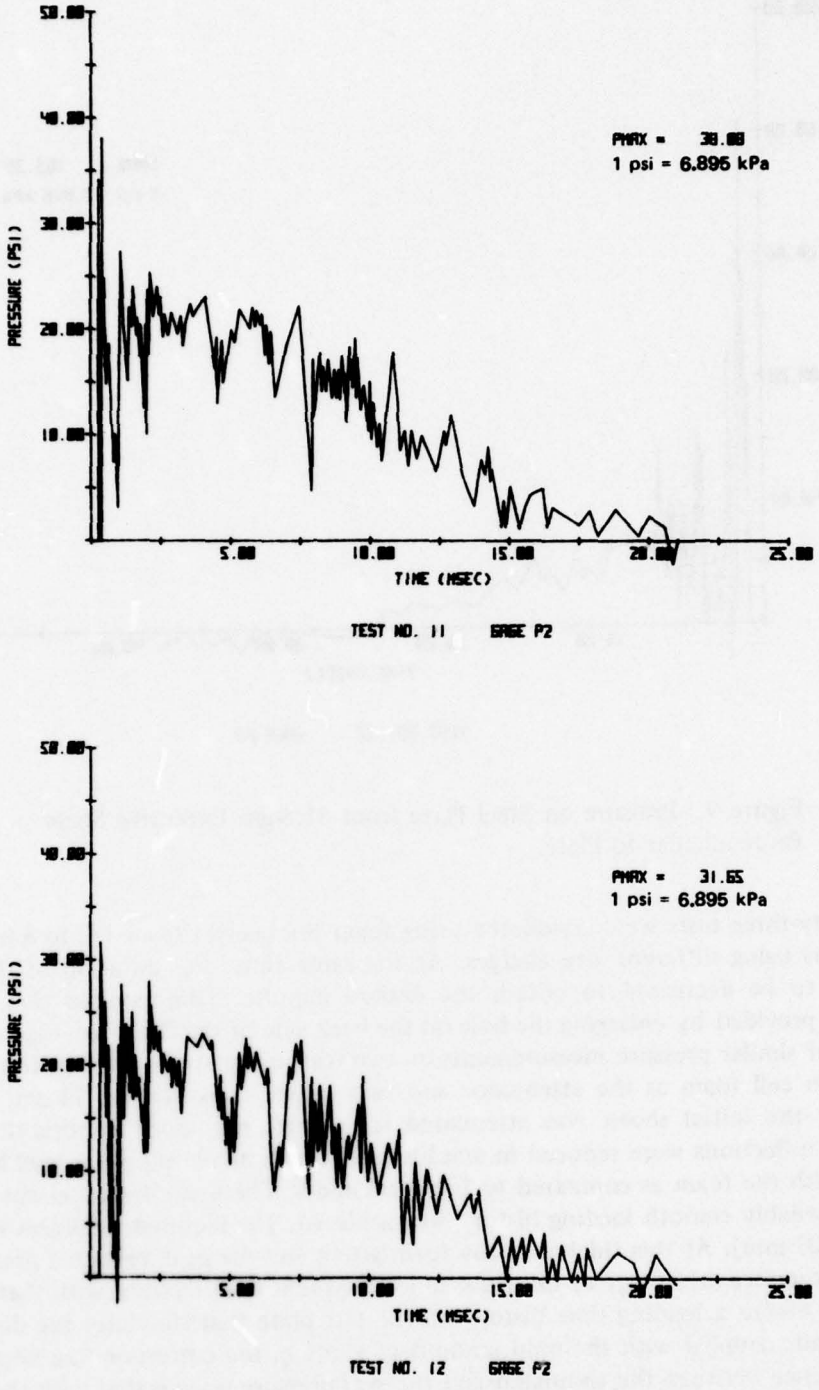

Figure 8. Gas Pressures Inside Vented Cubicle from 37-gm High Explosive Charges.

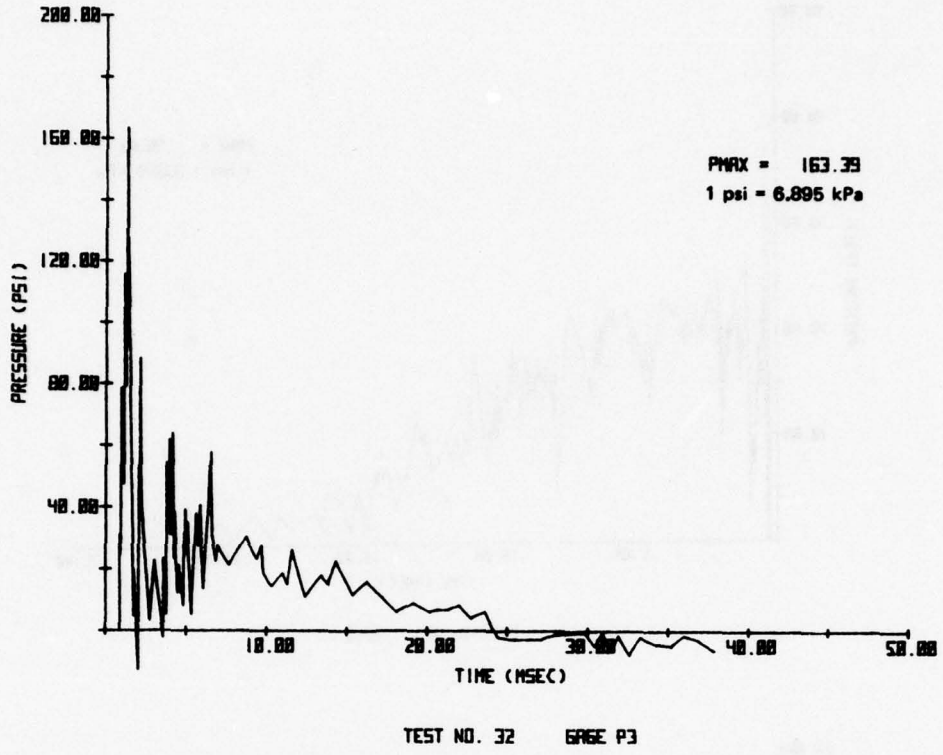

Figure 9. Pressure on Steel Plate from 81.5-gm Explosive Sheet Perpendicular to Plate.

Twenty-three tests were conducted using foam thicknesses from 1/2 to 8 inches (12.7 to 203 mm) using different size charges. At the same time, the duration of the pressure pulse had to be decreased to obtain the desired impulse. This required that additional venting be provided by enlarging the hole on the back side of the chamber. Figure 10 shows examples of similar pressure measurements on two tests using about 1 1/2 inches (38.1 mm) of the open cell foam as the attenuator and two charge sizes, 41 and 71 gm. The figure shows that the initial shock was attenuated somewhat, but more important, the large number of reflections were reduced in amplitude so that a much smoother load history was achieved with the foam as compared to Figures 6 and 9. The foam thickness was continued until a reasonably smooth loading history was achieved. The required thickness was around 8 inches (203 mm). At this thickness, the foam attenuates the peak reflected pressure quite well and integrates the energy of this peak and subsequent re-reflections with that of the gas pressure to create a loading time history on the test plate that simulates the desired peak pressures and, coupled with the right amount of venting, the corresponding impulses. The main difference between the simulated and the real pressure wave is that with the foam the rise time of the simulated peak pressure is 1 msec versus an almost infinitely small rise time for the real case. Another difference is that the decays of the peak pressure are somewhat different so that both the duration and the impulse cannot be simulated exactly.

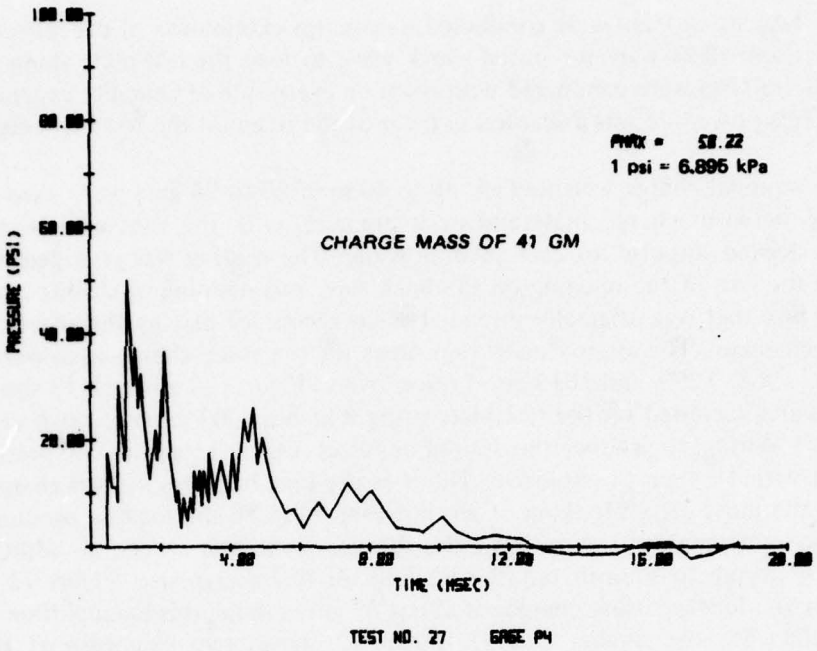

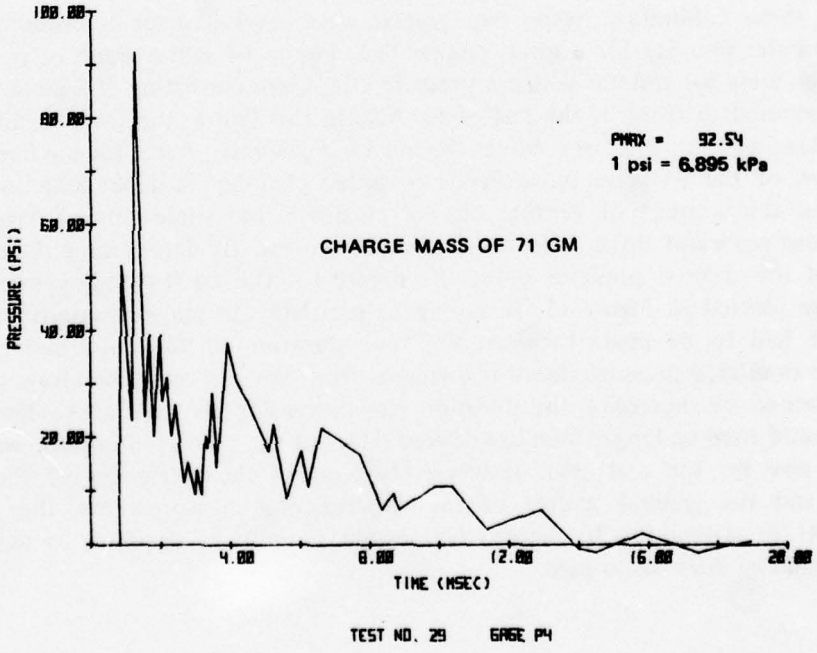

Figure 10. Pressure on Steel Plate Attenuated by 1 1/2 Inches (38.1 mm) of Foam.

Three tests using foam were conducted to attempt elimination of the reflections within the chamber and allow only the initial shock wave to load the test plate along with the gas pressure. These tests were conducted with foam on every side of chamber except against the test plate. This procedure was discarded in favor of the foam on the test plate only.

Three nominal charge weights (19, 38 to 40, and 80 to 94 gm) were used to obtain a relationship between charge mass and peak pressure, with the vent area being varied to obtain the desired impulse for each peak pressure. The venting was provided primarily by controlling the size of the opening on the back side, and opening or closing a hatch on the top of the box that was originally intended as an access for placing the sheet of explosive inside the chamber. The approximate vent areas for the three charge sizes were 150, 200, and 250 in^2 (968, 1290, and 1613 cm^2),respectively. Figures 11 through 13 show examples of the pressures recorded on the test plate using 8 inches (203 mm) of open cell foam and the necessary venting to produce the desired impulses. Figure 11 shows two pressure records from a test with 19.4 gm of explosive. The pressure-time histories for this charge size were, in general, the most ragged-looking of all; however, because the loading produced was not sufficient to permanently deform even the thinner aluminum sheets, no additional effort was spent in trying to smooth out the loading for this charge size. Figure 12 shows four examples of the loading using charges of about 39 gm in mass; this loading-time history was smoother than for the smaller charges. Figure 13 shows two examples of the pressure measured from charge masses of about 90 gm. These traces are very similar in appearance to the ones in Figure 12.

From these calibration tests, two graphs were developed for determining the peak pressure and the impulse for a given charge size. Figure 14 is the graph of peak pressure versus charge mass for tests in which a pressure attenuator consisting of 8 inches (203 mm) of foam was used in front of the test plate. Also in this figure, the three desired pressure points for loading the panels are shown. Figure 15 is a similar graph for the impulse. Since the duration of the pressure pulse inside a vented chamber is dependent on the initial pressure and the amount of venting on the chamber, the three sets of data shown in Figure 15 also represent three different degrees of venting. By determining the charge mass for each of the desired pressure points in Figure 14, the corresponding impulse values desired were plotted in Figure 15. In trying to simulate the real pressure-time history, a compromise had to be made between the time duration of the pulse and the impulse because the simulated pressure decay is different from the real one. Therefore, the impulse can be increased by increasing the duration (by decreasing the vent area). The simulated duration would then be longer than the desired one, but the simulated impulse would better match the one for the real case. However, because of the tolerances of the explosive properties and the general scatter of the experimental measurements, the amount of improvement in attempting to match the desired impulse as opposed to matching the duration would be difficult to gage.

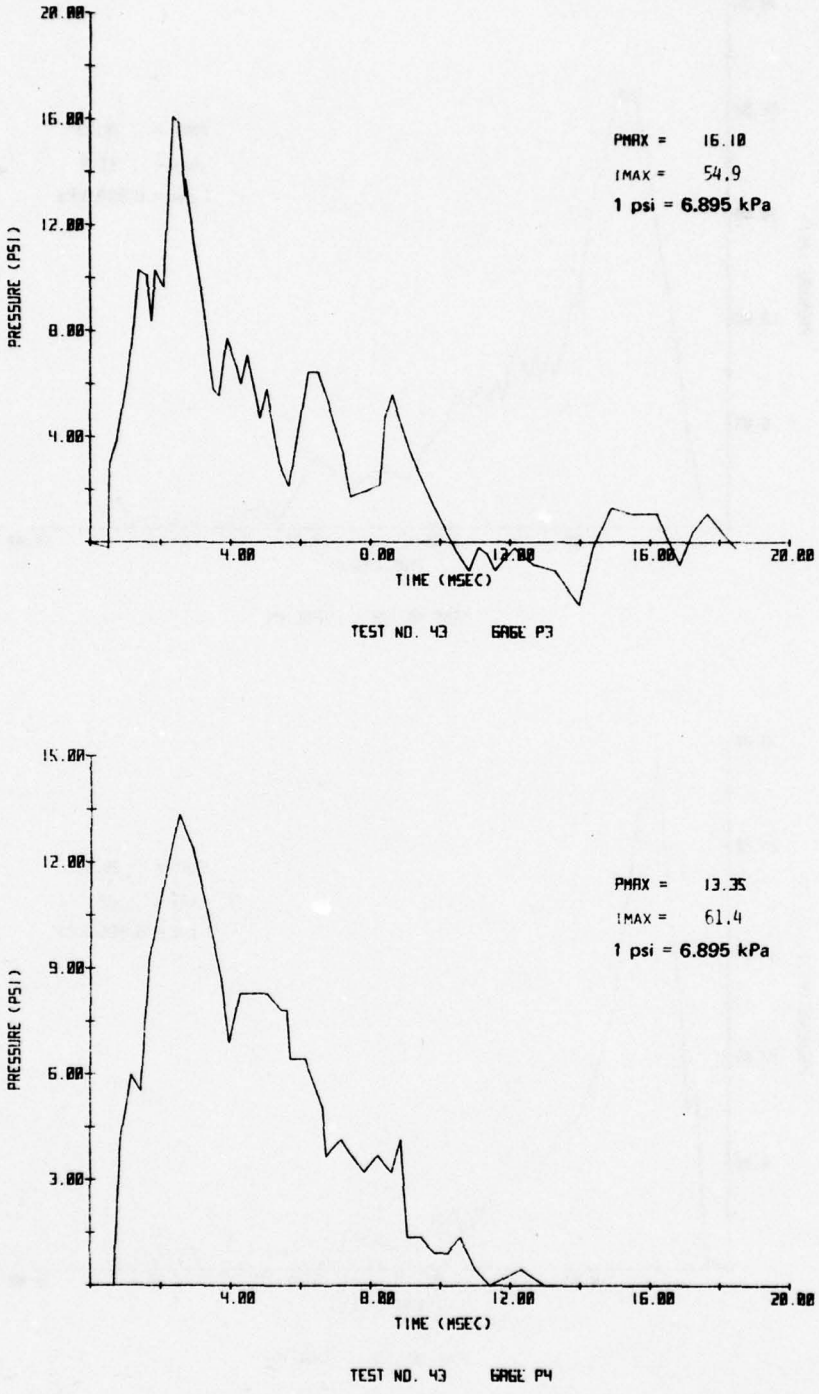

Figure 11. Pressure on Test Plate with 8 Inches (203 mm) of Foam Attenuator from 19.4-gm Charge.

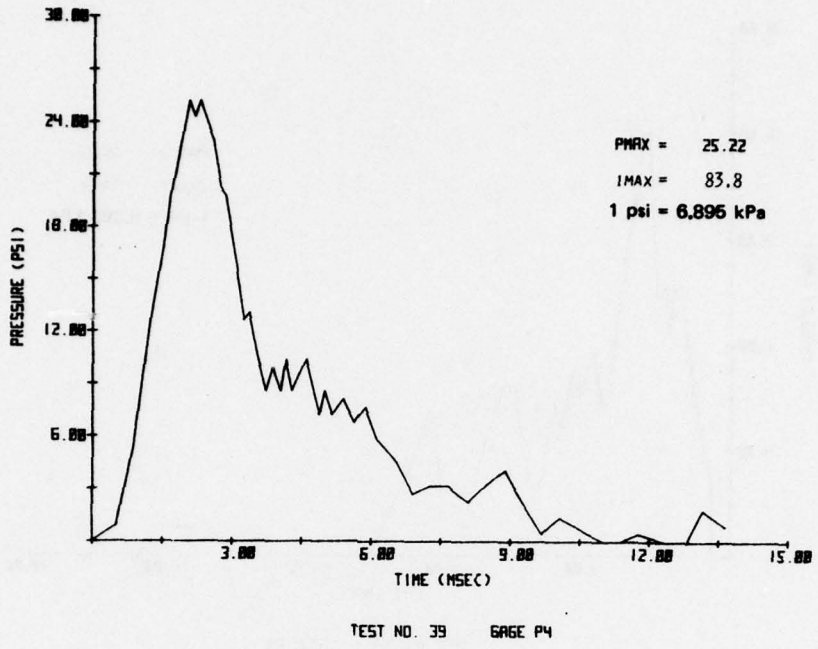

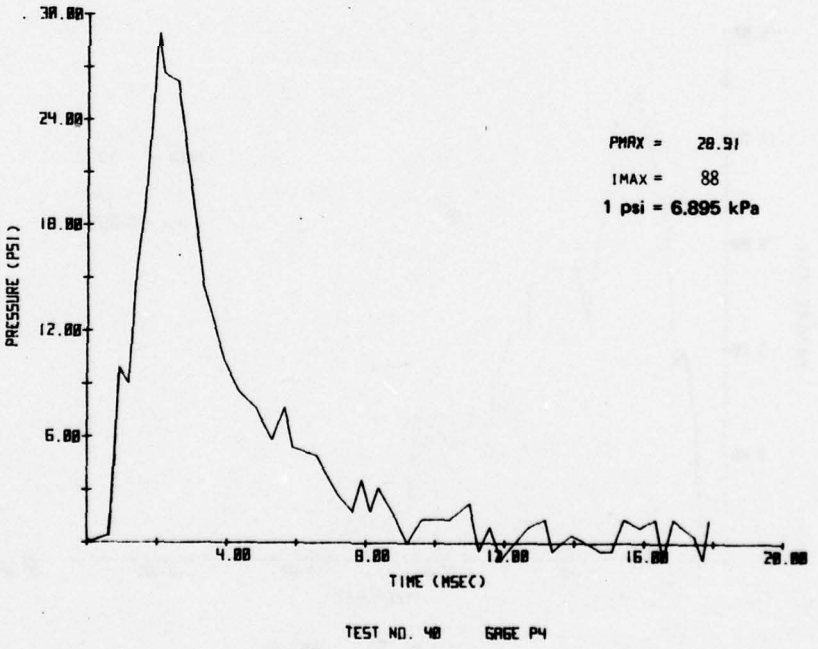

Figure 12. Pressure on Test Plate with 8 Inches (203 mm) of Foam Attenuator from 39-gm Charges.

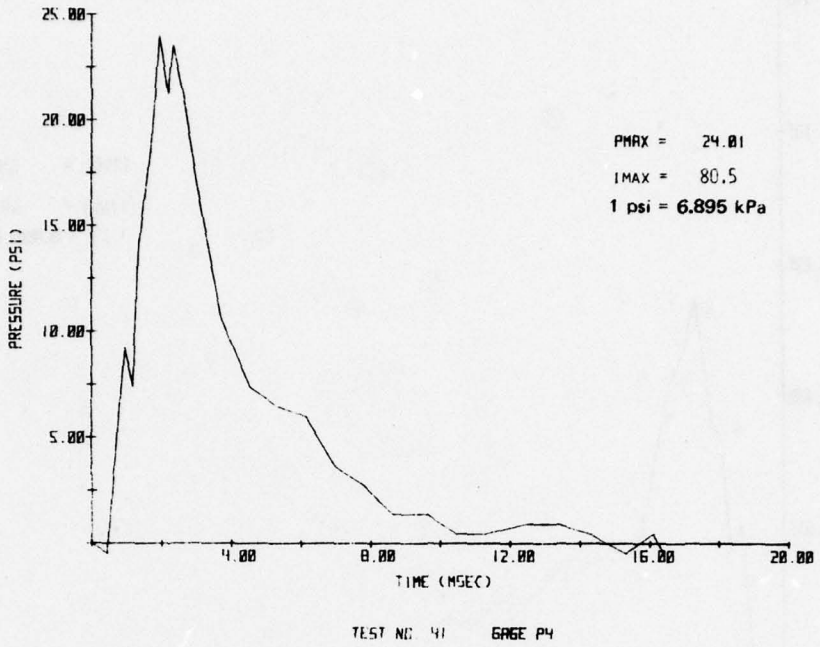

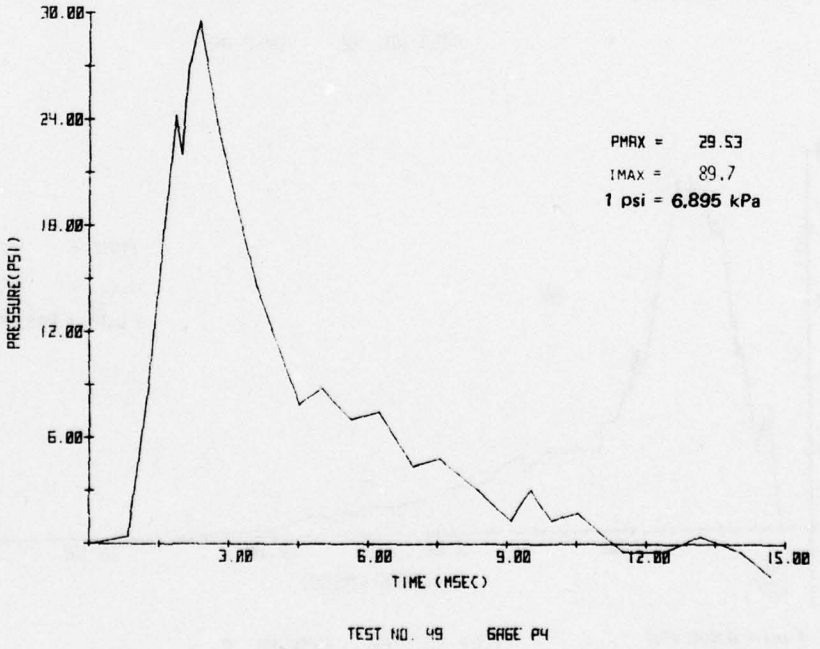

Figure 12. Pressure on Test Plate with 8 Inches (203 mm) of Foam Attenuator from 39-gm Charges. (Contd.)

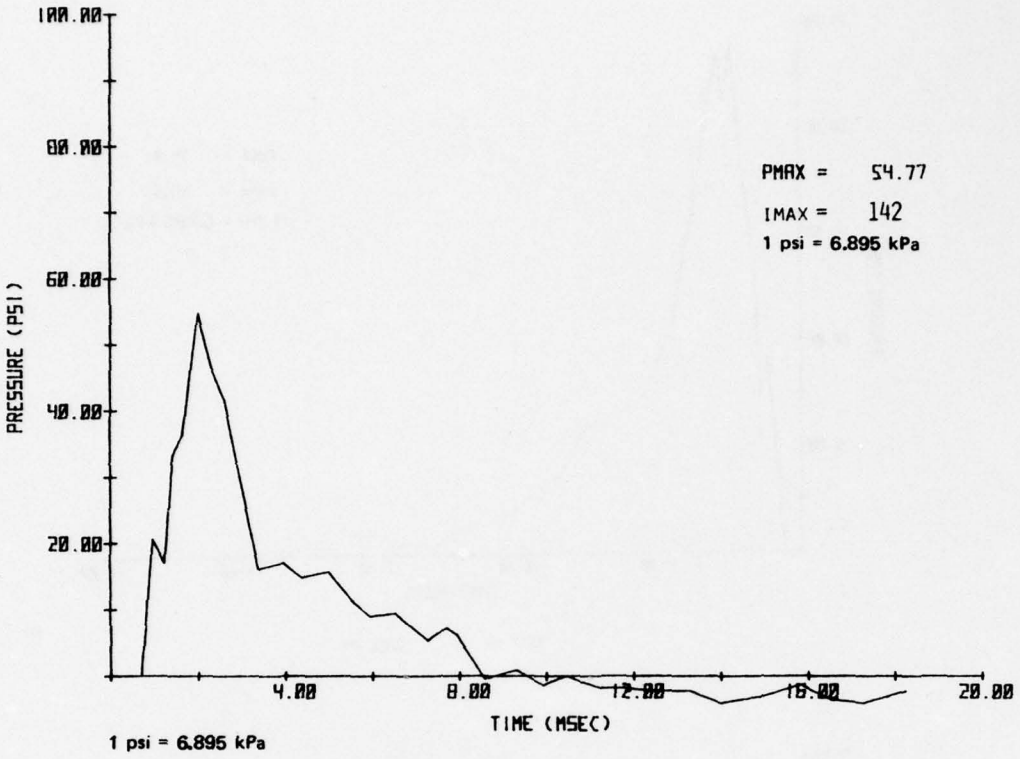

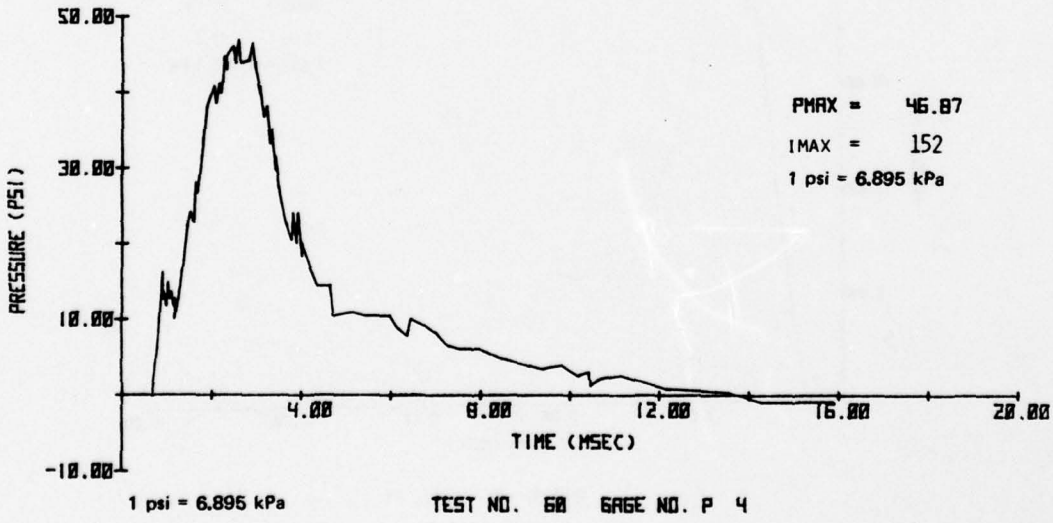

Figure 13. Pressure on Test Plate with 8 Inches (203 mm) of Foam Attenuator from 90-gm Charge.

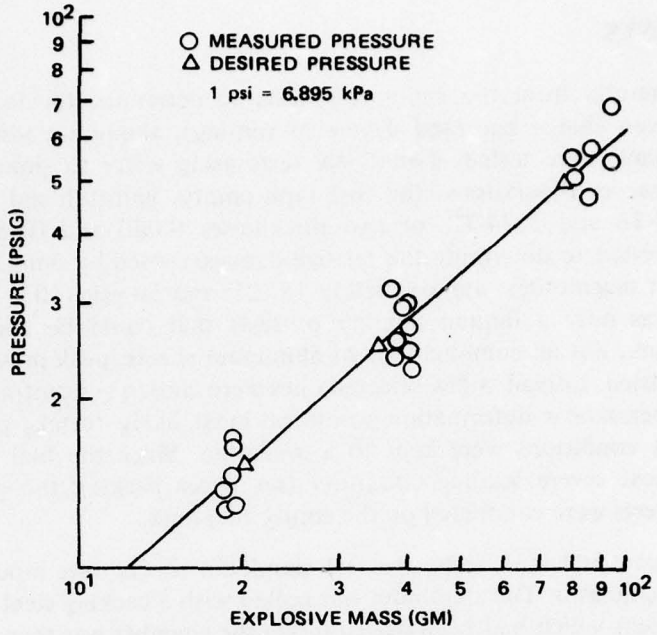

Figure 14. Peak Pressure on Test Plate with 8 Inches (203 mm) of Foam Attenuator as a Function of High Explosive Mass.

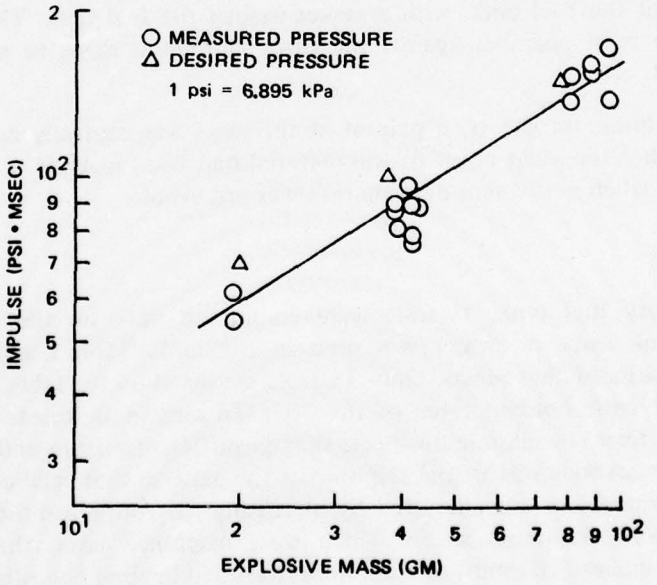

Figure 15. Impulse on Test Plate with 8 Inches (203 mm) of Foam Attenuator as a Function of High Explosive Mass.

FUEL TANK TESTS

Using the results from the calibration tests to determine the loading pressure and impulse for a given charge size (and degree of venting), aluminum test sheets simulating walls of a fuel tank were tested. Twenty-six tests using water to simulate the fuel were conducted in three configurations: the fuel tank empty, half-full, and full. Two types of aluminum, 7075-T6 and 2024-T3, of two thicknesses 0.040 and 0.080 inch (1.01 and 2.03 mm) were tested to determine the relative damage caused by simulated blast pressures of three different magnitudes: approximately 15, 25, and 50 psig (103, 172, and 345 kPa). Because there was only a limited number of tests that could be conducted using the simulated fuel tank, not all combinations of aluminum sheets, peak pressure, and fuel tank conditions were tried. Instead, a few selected ones were chosen concentrating on those cases in which some permanent deformation would be most likely to take place. Repeats of a given set of test conditions were kept to a minimum. Since the fuel tank being empty presented the most severe loading condition (no water backing the plate to attenuate response), more tests were conducted on the empty fuel tank.

For the empty fuel tank tests, the test aluminum sheets were mounted on the open side of the blast simulator. The aluminum was bolted with a backing steel frame as shown in Figure 16. The foam which had been placed inside the chamber was then moved against the aluminum panel but was not attached to the aluminum to minimize any mass effects on the response of the sheet. During tests in which the fuel tank was either full or half-full of water, the fuel tank frame was used to support the front and back replaceable aluminum walls. The back wall was bolted to the flange on the fuel tank with a gasket on the inside and a backing steel frame on the outside. The front plate was bolted between the flanges of the blast tank and the fuel tank, with a gasket against the fuel tank. The foam was again placed inside the blast chamber against the front aluminum sheet to obtain the desired pressure-time load.

On all the aluminum sheets, a pair of strain gages was centrally mounted for use in determining whether the yield point of the material had been reached at the center of the wall in those tests when permanent deformation was not visible.

Empty Tank Tests

For the empty fuel tank, 17 tests were conducted only on the front wall of the simulated fuel tank since no water was used in the tank. Table 1 summarizes the test conditions and results of these tests. Only 11 tests are listed on the table because problems were encountered with holding three of the 7075-T6 aluminum sheets against the blast chamber. In these tests, the aluminum sheets slipped sufficiently from under the hold down frame and bolts to severely distort the response of the plate so that valid comparisons could not be made. This problem was alleviated by increasing the torque on the bolts, and in the case of the 2024-T3 aluminum sheets which were machined later, the plates were cut oversize so that 4 inches (102 mm) of aluminum extended beyond the edge of the blast and fuel tank flanges. The other three tests were fired using different sizes of foam lining the chamber before it was decided to go with the 8 inches (203 mm) on the test plates. Thus, the results of these three tests are not comparable with those shown in Table 1.

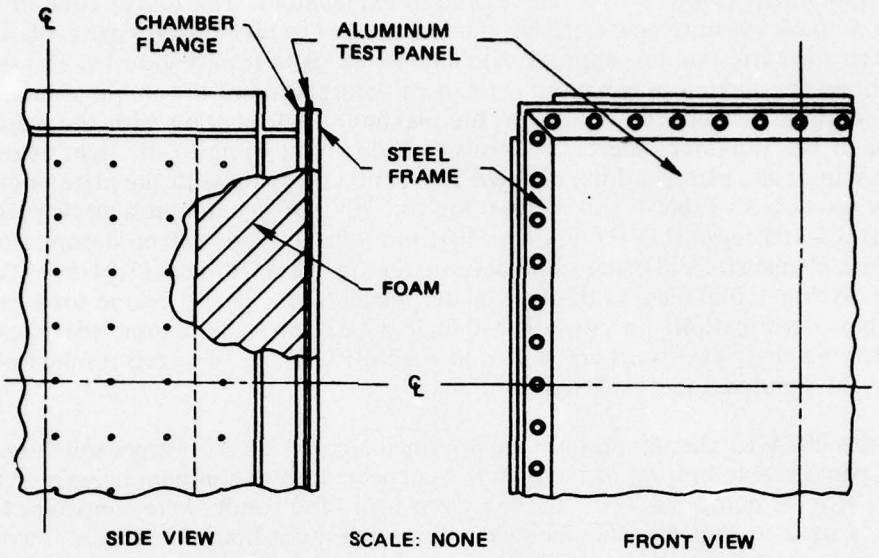

Figure 16. Aluminum Test Panel and Foam Installation on Blast Chamber for Empty Fuel Tank Tests.

Table 1. Empty Fuel Tank Tests[a].

Plate	Thickness, in.	Charge mass, gm	Approximate peak pressure, psig[b]	Approximate impulse, psi • msec[c]	Measurable maximum deformation, in.	Location of maximum deformation, in.	
						X	Y
7075-T6 aluminum plate material							
1	0.040	20.6	15	60	None		
2	0.040	36.2	25	87	0.15	0.0	0.0
3	0.080	40.3	28	92	None		
6	0.080	87.6	56	151	1.51	0.0	0.0
10	0.080	79.4	51	143	1.51	1.0	0.5
2024-T3 aluminum plate material							
24	0.040	39.0	27	90	1.83	0.0	0.0
23	0.080	40.3	28	92	1.13	0.0	1.0
15	0.080	77.9	50	140	1.93	2.0	0.0
16	0.080	77.6	50	140	2.08	2.8	0.5
17	0.040	77.0	50	140	3.23	1.5	1.0
18	0.040	76.7	50	140	3.28	0.2	1.5

[a] 1 inch = 25.4 mm; 1 psi = 6.895 kPa.
[b] See Figure 14.
[c] See Figure 15.

The first three columns in Table 1 are self-explanatory. The fourth column lists the approximate peak pressure generated by the charge used as taken from Figure 14. The fifth column lists the corresponding approximate impulse as taken from Figure 15. The following column shows the maximum measured permanent deformation of the aluminum sheets. The last two columns give the coordinates of the maximum deformation with the origin being the center of the aluminum sheets, the positive X-direction being to the right as one faces the bulge side of the plate, and the positive Y-direction being up with the plate oriented the same way as tested. Table 1 shows that for the 7075-T6 aluminum a peak pressure of 15 psig (103.4 kPa) against a 0.040-inch (1.01 mm) sheet produced no deformation. The intermediate charge size did cause some deformation to the 0.040-inch (1.01-mm) thickness but none to the 0.080-inch (2.03-mm) plate. Finally, the larger charge used produced considerable deformation on two 0.080 inch (2.03 mm) aluminum specimens. The deformation on these two walls are shown in Figure 17. These two tests resulted in similar damage to the simulated fuel tank walls.

For the 2024-T3 aluminum, only the intermediate and largest charges were used which produced considerable bulging of the plates. As expected, this aluminum being more ductile than the 7075-T6, deformed more under a given load. The results were consistent for both charge sizes used in that the thinner sheets deformed more than the thicker. Two sets of repeated test conditions using the large charges were fired, one set with each of the thicknesses used. In both cases, excellent repeatability of the damage was found. Figure 18 shows the walls loaded with the intermediate charges and Figure 19 those loaded with the large charges. Some of the sheets tested were instrumented with a two element strain gage rosette centrally located. One element was oriented vertically and the other horizontally. Because of the high accelerations induced on the strain gage wires and in most cases the severe deformations, the strain measurements were not too successful, particularly on the empty tank tests. In some cases, strain levels in the order of 3000 to 4000 μin/in were recorded before the leads were severed. These levels are under the nominal yield value of both types of aluminum and for the walls that deformed permanently the strain levels reached were obviously much higher.

Half-Full Tank Tests

Five tests were conducted with the simulated fuel tank half-full of water, three using 7075-T6 aluminum and two using the 2024-T3 aluminum. None of the 7075-T6 sheets deformed plastically. Strain measurements were obtained on these tests. Figures 20 and 21 show the data for two of the 7075-T6 tests in which the only difference in the setup was the charge size. The top trace in each figure is the vertical measurement and the bottom trace the horizontal measurement. Because the plates were backed by water half-way up, the strains at the center of the plate would have been of lower value than those further up the plate along the vertical center line. Nevertheless, the central measurements provided an indication of how far the plate was from reaching its yield point near the center. Furthermore, with the water helping to attenuate the high-shocks being experienced by the strain gage wires, the gages survived more often and for longer times than if no water had been there. The corresponding strain records shown in Figures 20 and 21 are similar except for amplitude. The larger charge produced the higher strain levels with the maximum strain recorded corresponding to a stress of about 34,000 psi (234 MPa), well below the minimum yield stress of 73,000 psi (503 MPa) for 7075-T6 aluminum.

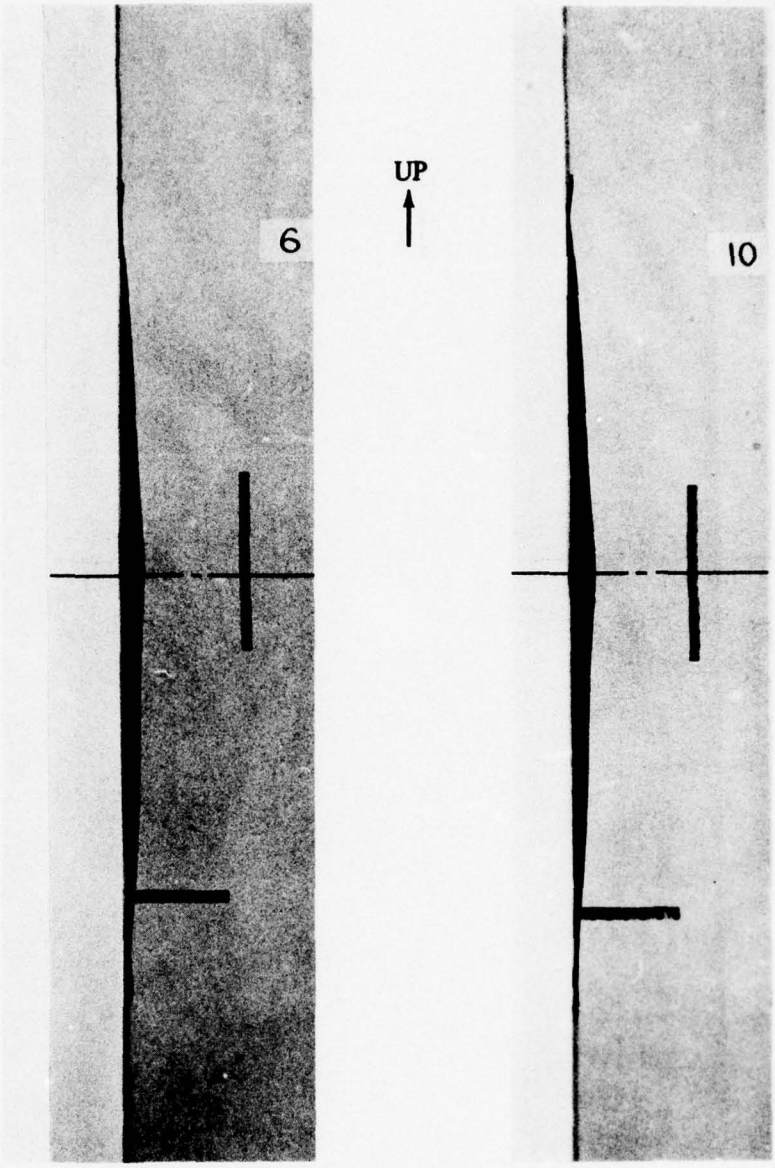

(a) 88-gm charge (b) 79-gm charge

Figure 17. Side View of 0.080 Inch (2.03 mm). 7075-T6 Aluminum Walls Tested with Empty Fuel Tank.

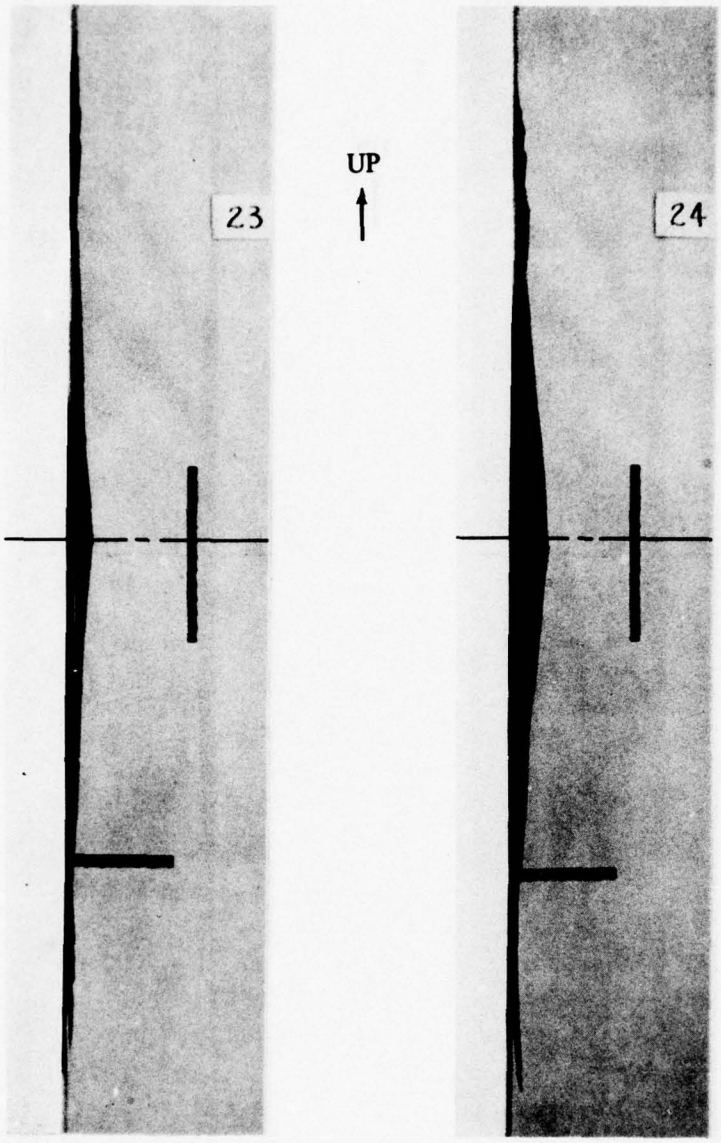

(a) 0.080-inch (2.03-mm)wall

(b) 0.040-inch (1.01-mm) wall

Figure 18. Side View of 2024-T3 Aluminum Walls Tested with Empty Fuel Tank and 40-gm Sheet Explosive.

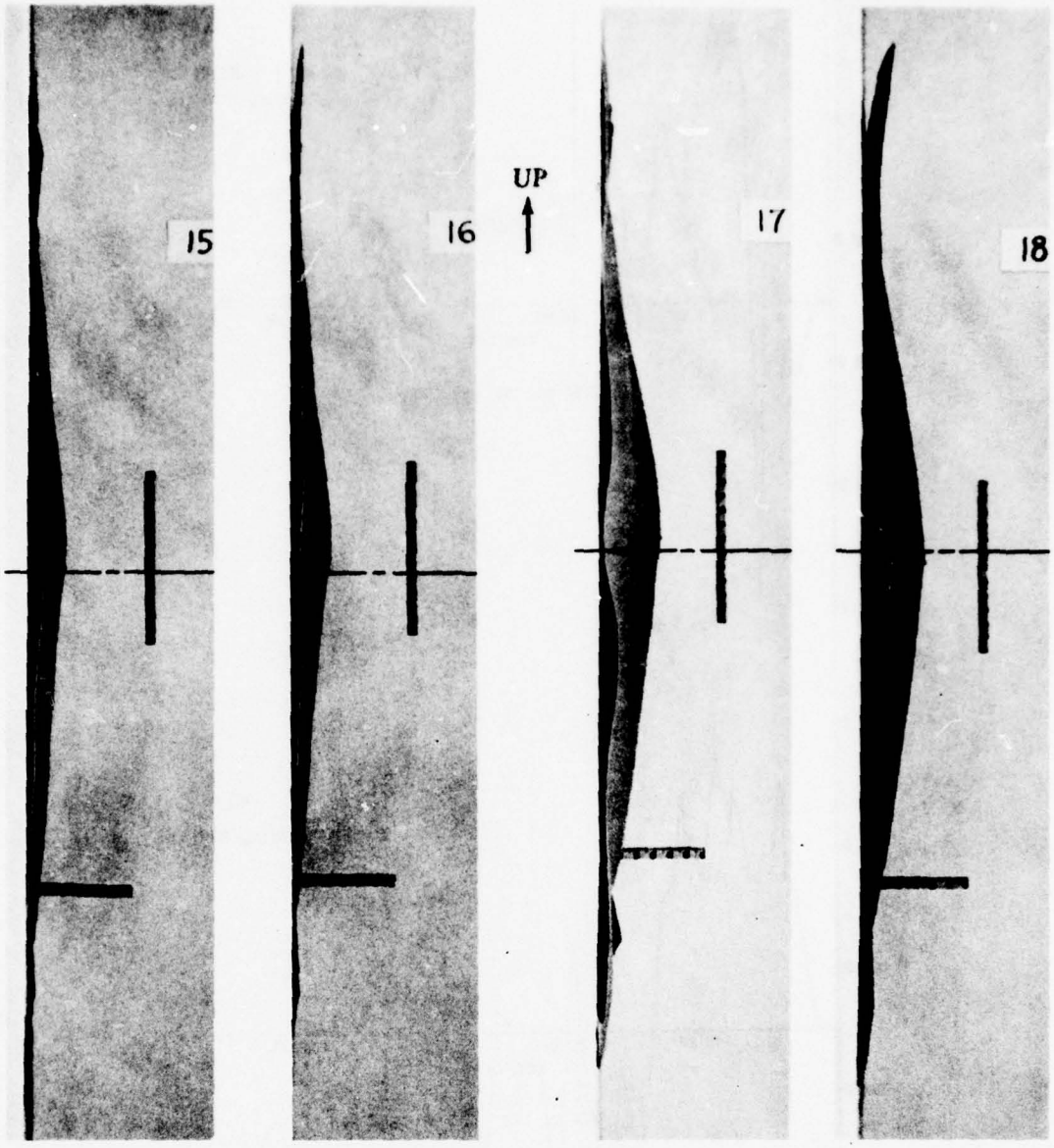

(a) 0.080-inch (2.03-mm) walls

(b) 0.040-inch (1.01-mm) walls

Figure 19. Side View of 2024-T3 Aluminum Walls Tested with Empty Fuel Tank and 78-gm Sheet Explosive.

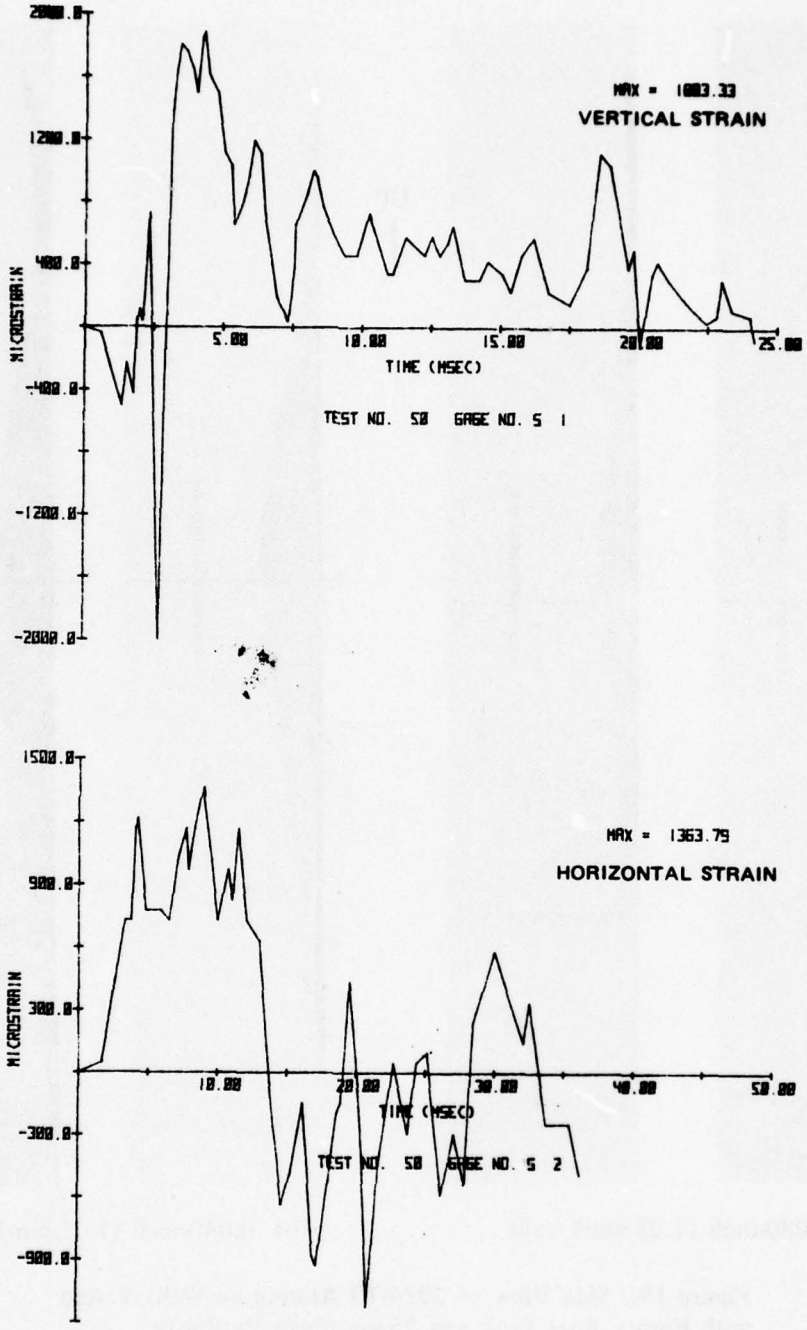

Figure 20. Strain Data from 40-gm Explosive Sheet Loading 0.080 Inch (2.03 mm), 7075-T6 Aluminum Plate with Fuel Tank Half-Full of Water.

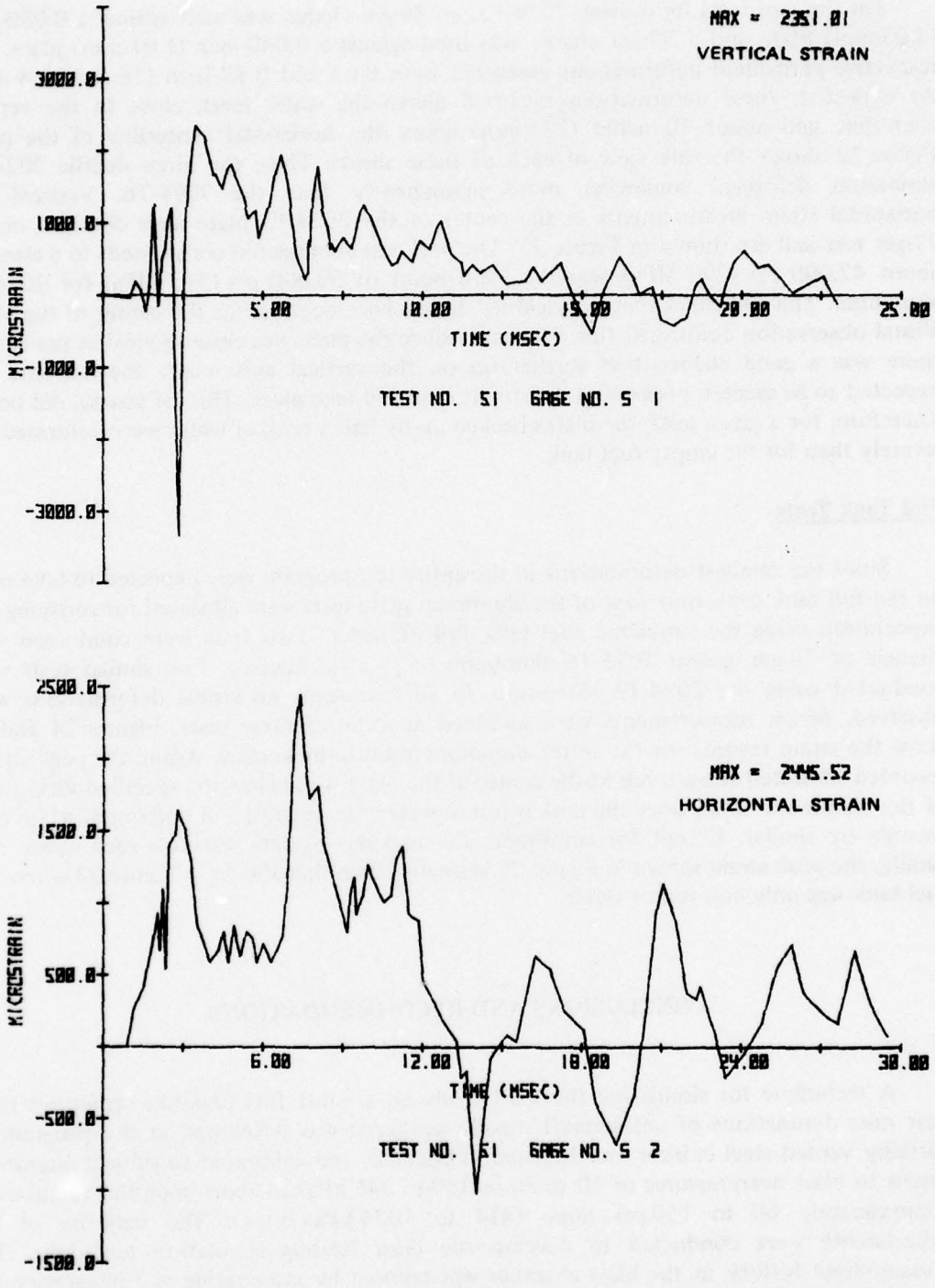

Figure 21. Strain Data from 82-gm Explosive Sheet Loading 0.080 Inch (2.03 mm), 7075-T6 Aluminum Plate with Fuel Tank Half-Full of Water.

On the two tests fired using 2024-T3, an 80-gm charge was used against a 0.080-inch (2.03-mm) plate and a 77-gm charge was used against a 0.040-inch (1.01-mm) plate. The respective permanent deformations measured were 0.63 and 0.88 inch (16 and 22.4 mm). As expected, these deformations occurred above the water level, close to the vertical centerline and about 10 inches (254 mm) above the horizontal centerline of the plate. Figure 22 shows the side view of each of these sheets. Thus, the more ductile 2024-T3 aluminum deformed somewhat more permanently than the 7075-T6. Vertical and horizontal strain measurements at the center of the 2024-T3 plate were obtained on the 77-gm test and are shown in Figure 23. The peak strain measured corresponds to a stress of about 42,000 psi (290 MPa) near the yield point of 50,000 psi (345 MPa) for 2024-T3 aluminum. This indicated that no yielding should have occurred at the center of the plate. Visual observation confirmed this. However, since the plate was close to yield at the center, there was a good chance that further up on the vertical axis where the response was expected to be greater, permanent deformation would take place. This, of course, did occur. Therefore, for a given load, the plates backed up by half a tank of water were deformed less severely than for the empty fuel tank.

Full Tank Tests

Since the smallest deformations in the entire test program were expected to take place on the full tank tests, only four of the aluminum plate tests were allocated for verifying this expectation using the simulated fuel tank full of water. Two tests were conducted with charges of 78 gm against 7075-T6 aluminum of two thicknesses. Two similar tests were conducted using the 2024-T3 aluminum. In all four tests, no visible deformations were observed. Strain measurements were obtained in some of these tests. Figures 24 and 25 show the strain records for the softer aluminum in both thicknesses. Again, the peak strains recorded indicated stress levels at the center of the plate well below the specified yield point of the aluminum. Also, since the tank is full of water, the vertical and horizontal strain-time records are similar. Except for amplitude, the two sets of data resemble each other. And finally, the peak strain shown in Figure 25 is smaller than that shown in Figure 23 where the fuel tank was only half-full of water.

CONCLUSIONS AND RECOMMENDATIONS

A technique for simulating the blast loads on aircraft fuel tank-like structures from near miss detonations of anti-aircraft missile warheads was developed in this program. A partially vented steel cubicle was designed, fabricated, and calibrated to subject aluminum panels to blast overpressures of 10 to 50 psi (69 to 345 kPa) and corresponding impulses of approximately 60 to 150 psi • msec (414 to 1034 kPa • msec). The majority of the experiments were conducted to develop the blast loading simulation technique. The pressure-time history in the blast chamber was tailored by attenuating and integrating the initial shock pressure and subsequent reflections with open cell foam to obtain a relatively smooth pressure rise and initial decay which blended with the longer duration, lower

amplitude gas pressure in the chamber. The duration was controlled by the amount of venting allowed and this was set so that a compromise value of impulse and duration was achieved which closely matched the real situation being simulated. Two graphs (Figures 14 and 15) resulted from the calibration tests. Figure 14 relates the peak pressure to the size of the explosive detonated in the chamber. Using this graph, the peak pressure loading a test plate through a pressure attenuator consisting of 8 inches (203 mm) of open cell foam can be estimated for a given charge mass. Figure 15 yields an estimate of the impulse produced by the high-explosive detonation.

Using these two graphs to determine the charge sizes required for a desired given load, a limited number of experiments were conducted on a simulated fuel tank. A steel tank with removable aluminum ends was designed and built to test simulated fuel tank walls of 7075-T6 and 2024-T3 aluminum in two thicknesses, 0.040 and 0.080 inch (1.01 and 2.03 mm). Three different fuel tank conditions were tested using water as the liquid in the tank: an empty tank, a half-full tank, and a full tank. As expected, the more ductile 2024-T3 aluminum deformed more under a given load than the 7075-T6. Also, for each type of aluminum, the empty tank tests produced the largest deformations since no water was present to attenuate the response. In the case of the 7075-T6 sheets, significant permanent deformations of about 1.5 inches (38.1 mm) were achieved only at peak overpressures of about 50 psi (345 kPa) with the fuel tank empty. Very little or no deformations were produced by the smaller charges used or with water in the fuel tank. On the other hand, the 2024-T3 walls had deformations greater than 1 inch (25.4 mm) on the empty tank tests from the intermediate overpressure of about 27 psi (186 kPa) and the higher pressure of 50 psi (345 kPa) which caused deformations in excess of 3 inches (76 mm) on the thinner aluminum panels. The half-full fuel tank tests using the thinner 2024-T3 aluminum walls had deformations of 0.88 inch (22.4 mm) from pressures of 40 psi (276 kPa). None of the full tank tests had measurable deformations.

The blast simulator has been calibrated and shown to produce fairly repeatable pressures and impulses at three charge weights. Any pressure and impulse within this range can be estimated using the results of this program. The simulated fuel tank tests conducted showed that blast pressures alone will cause significant structural damage only to very light, brittle structure similar to unstiffened 0.040-inch (1.01-mm) 7075-T6 aluminum. Permanent deformation of aircraft fuel tank walls, short of failure and rupture, is not a serious problem. Damage to light structure other than fuel tank walls, such as control surfaces, could be a significant factor but is beyond the scope of this effort. However, since blast is only one of the damage mechanisms from near-miss warhead detonations, a considerable testing effort should be conducted in which high velocity fragments (another major threat) is investigated alone and coupled with the blast threat to determine whether accurate simulation of missile warhead near-miss detonations to simulated fuel tanks must include blast effects. The blast simulator was designed and built so that fragments could be launched through it. Thus, this structure can be used to conduct the coupled fragment and blast tests.

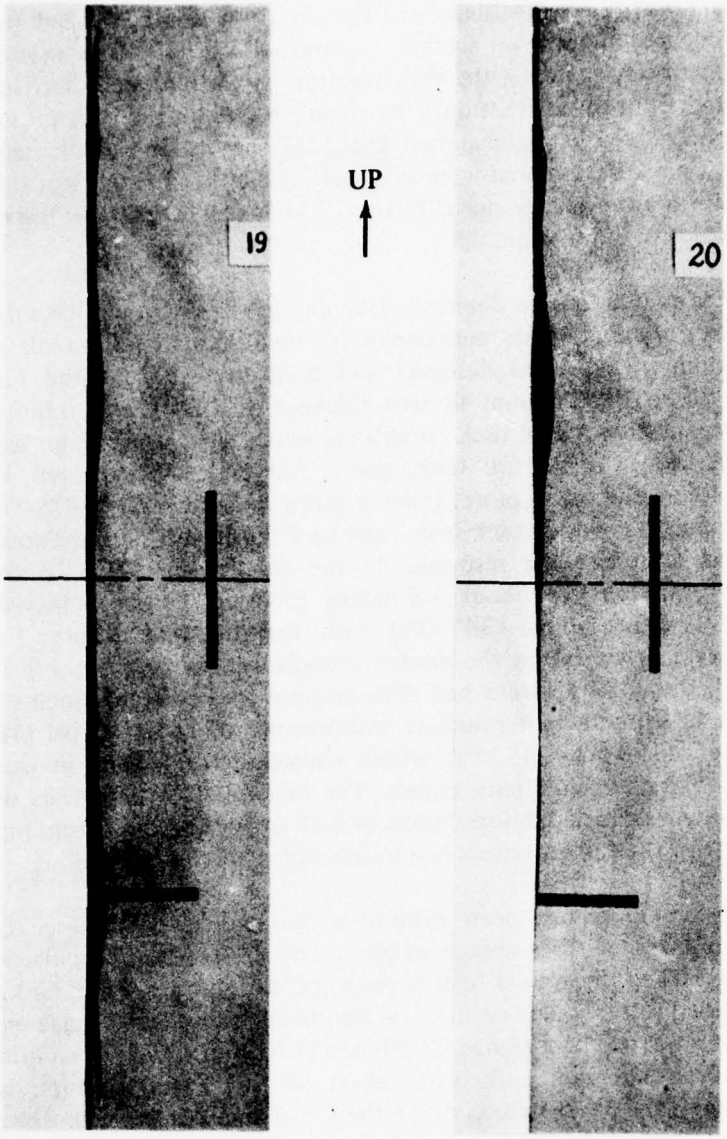

(a) 0.080-inch (2.03-mm) wall 80-gm charge

(b) 0.040-inch (1.01-mm) wall 77-gm charge

Figure 22. Side View of 2024-T3 Aluminum Walls Tested with Fuel Tank Half-Full of Water.

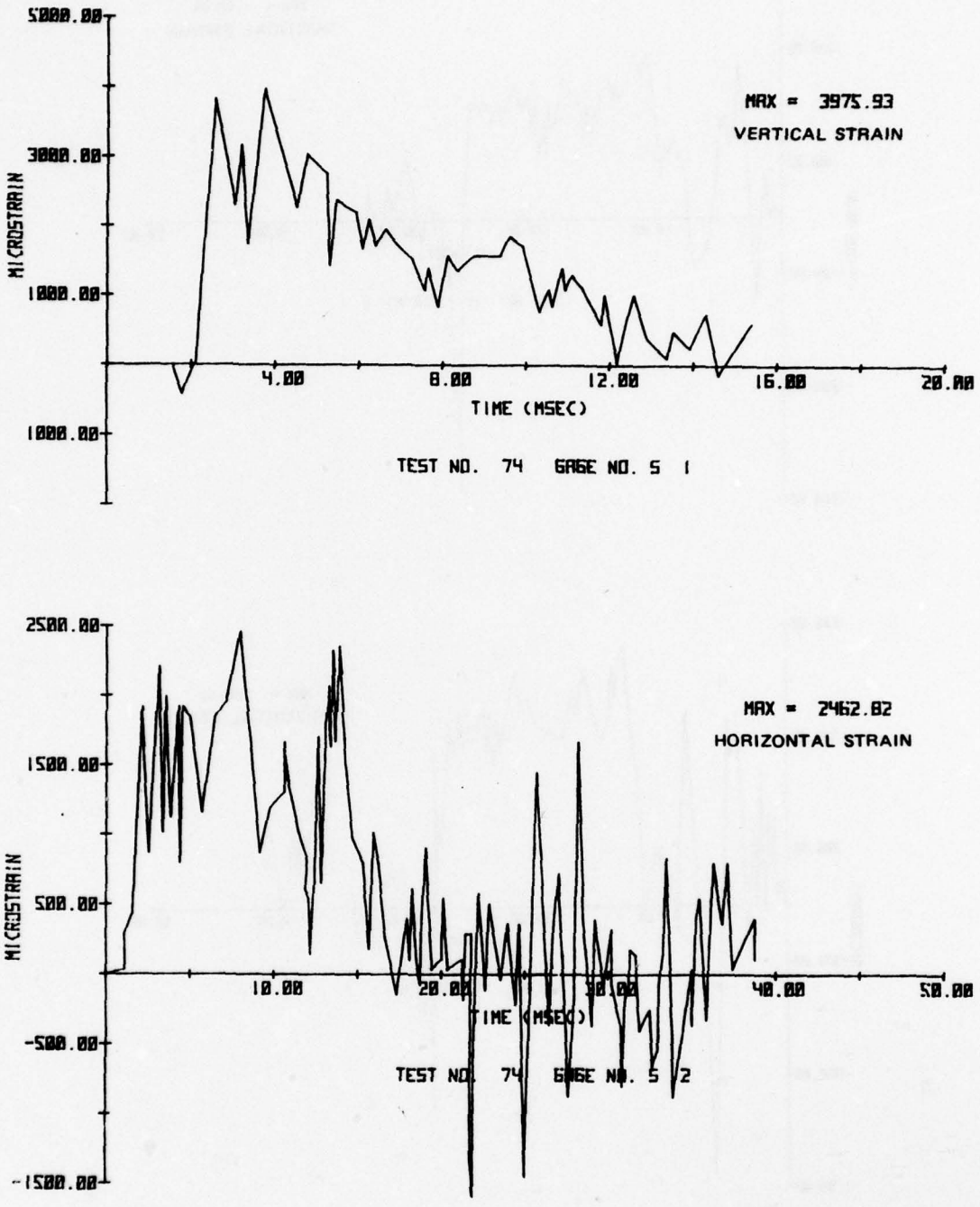

Figure 23. Strain Data from 77-gm Explosive Sheet Loading 0.040 Inch (1.01 mm), 2024-T3 Aluminum Plate with Fuel Tank Half-Full of Water.

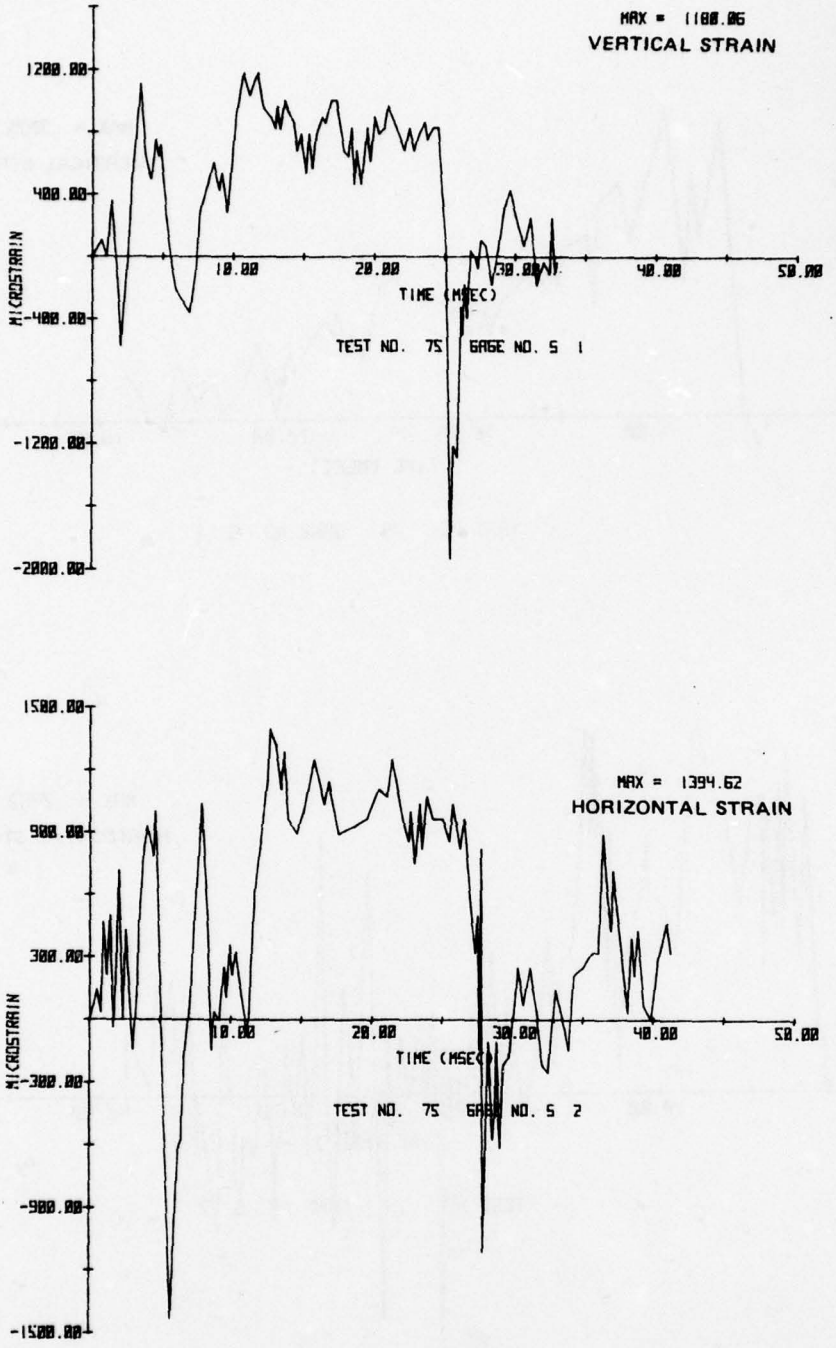

Figure 24. Strain Data from 77-gm Explosive Sheet Loading 0.080 Inch (2.03 mm), 2024-T3 Aluminum Plate with Fuel Tank Full of Water.

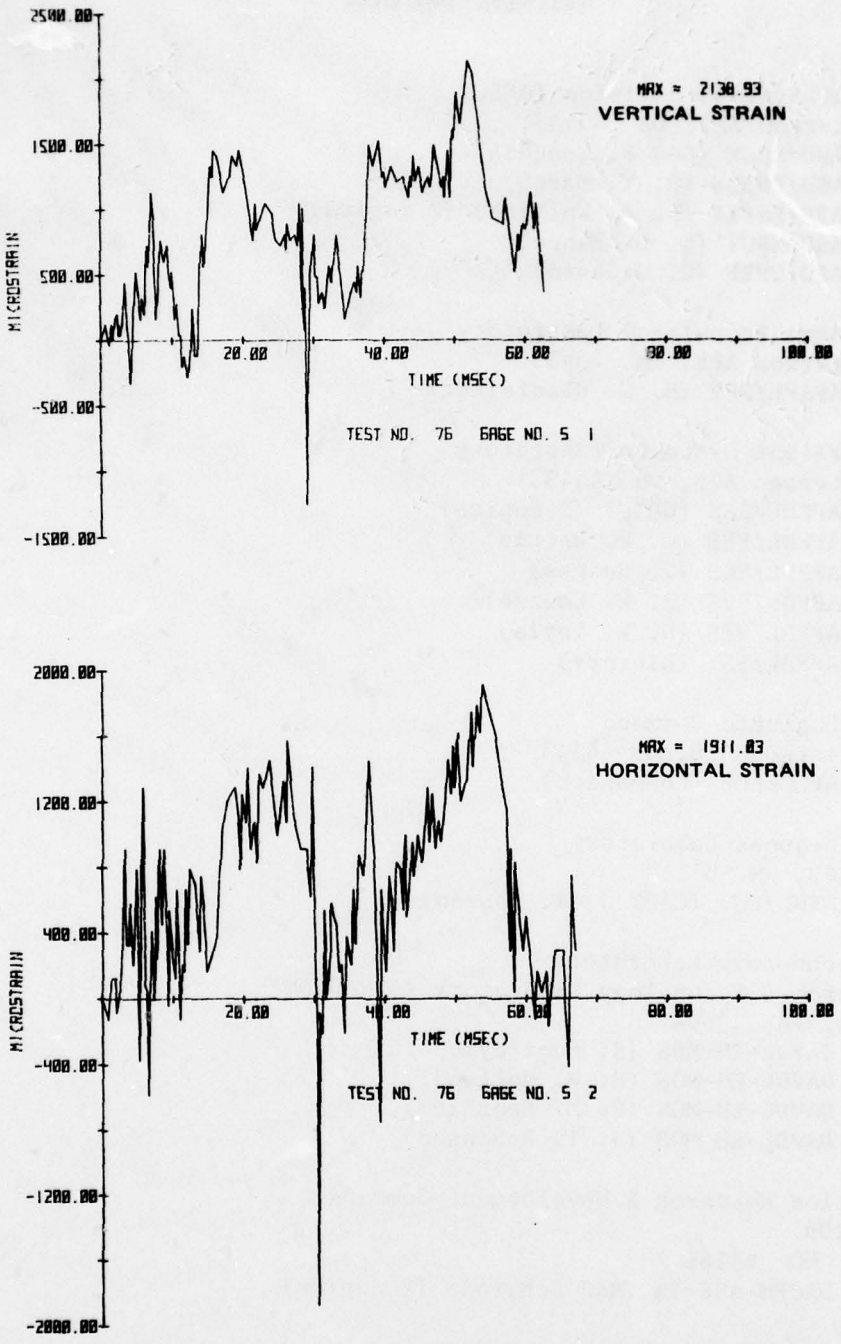

Figure 25. Strain Data from 77-gm Explosive Sheet Loading 0.040 Inch (1.01 mm), 2024-T3 Aluminum Plate with Fuel Tank Full of Water.

DISTRIBUTION LIST

Aeronautical Systems Division (AFSC)
Wright-Patterson AFB, OH 45433
Attn: ASD/ACCX (MAJ F. Munguia)
Attn: ASD/ENESS (P. T. Marth)
Attn: ASD/ENFTV (D. J. Wallick) (2 copies)
Attn: ASD/XROT (G. B. Bennett)
Attn: ASD/YPEF (C. Gebhard)

Air Force Aero Propulsion Laboratory
Wright-Patterson AFB, OH 45433
Attn: AFAPL/SFH (R. G. Clodfelter)

Air Force Flight Dynamics Laboratory
Wright-Patterson AFB, OH 45433
Attn: AFFDL/FES (CDIC) (2 copies)
Attn: AFFDL/FES (C. W. Harris)
Attn: AFFDL/FES (J. Hodges)
Attn: AFFDL/FES (R. W. Lauzze)
Attn: AFFDL/FES (D. W. Voyls)
Attn: AFFDL/TST (Library)

Air Force Logistic Command
Wright-Patterson AFB, OH 45433
Attn: AFLC/LOE (Commander)

Air Force Weapons Laboratory
Kirtland AFB, NM 87117
Attn: AFWL/PGV (CAPT J. K. Carson)

Applied Technology Laboratory
Army Research & Technology Laboratory (AVRADCOM)
Ft. Eustis, VA 23604
Attn: DAVDL-EU-MOS (S. Pociluyko)
Attn: DAVDL-EU-MOS (H. W. Holland)
Attn: DAVDL-EU-MOS (C. M. Pedriani)
Attn: DAVDL-EU-MOS (J. T. Robinson)

Army Aviation Research & Development Command
P.O. Box 209
St. Louis, MO 63166
Attn: DRCPM-ASE-TM (MAJ Schwend) (2 copies)

Army Ballistic Research Laboratories
Aberdeen Proving Ground, MD 21005
Attn: DRXBR-VL (D. W. Mowrer)

Army Foreign Science and Technology Center
220 Seventh St., NE
Charlottesville, VA 22901
Attn: DRXST-BA3 (E. R. McInturff)

Army Materials and Mechanics Research Center
Watertown, MA 02172
Attn: DRXMR-PL (M. M. Murphy) (2 copies)
Attn: DRXMR-RD (R. W. Lewis)

Army Materiel Systems Analysis Activity
Aberdeen Proving Ground, MD 21005
Attn: DRXSY-J

Combat Development Experimentation Command
155th Aviation Co. (Attack Helicopter Group)
Fort Ord, CA 93941
Attn: ATEC-ATK

Defense Documentation Center
Cameron Station, Bldg. 5
Alexandria, VA 22314
Attn: DDC-TCA (12 copies)

Defense Systems Management College
Ft. Belvoir, VA 22060
Attn: W. Schmidt

Department of Transportation - FAA
2100 Second St., SW, Rm 1400C
Washington, DC 20591
Attn: ARD-520 (R. A. Kirsch)

Foreign Technology Division (AFSC)
Wright-Patterson AFB, OH 45433
Attn: FTD/SDNS-3 (LT Saylor/73041)

HQ Air Logistics Command
McClellan AFB, CA 95652
Attn: SM/MMSRBC (D. E. Snider)

HQ SAC
Offutt AFB, NB 68113
Attn: NRI/STINFO Library

Marine Corps Development Center
Quantico, VA 22134
Attn: D-091 (LT COL J. Givan)

NASA - Ames Research Center
Army Air Mobility R&D Laboratory
Mail Stop 207-5
Moffett Field, CA 94035
Attn: DAVDL-AS (V. L. J. Di Rito)

NASA - Lewis Research Center
21000 Brookpark Rd.
Mail Stop 500-202
Cleveland, OH 44135
Attn: Library (D. Morris)

Naval Air Development Center
Warminster, PA 18974
Attn: Code 2012 (M. C. Mitchell)
Attn: Code 6013: JJK
Attn: Code 6099 (R. A. Ritter)

Naval Air Propulsion Test Center
P.O. Box 7176
Trenton, NJ 08628
Attn: PE42 (R. W. Vizzinni)

Naval Air Systems
Airtevron One
Patuxent River MD 20653
Attn: LT R. N. Freedman

Naval Air Systems Command
Washington, DC 20361
Attn: AIR-330B (E. A. Lichtman)
Attn: AIR-52014 (L. Sztan)
Attn: AIR-5204A (D. Atkinson) (2 copies)
Attn: AIR-5204J (LT COL R. T. Remers)
Attn: AIR-5303
Attn: AIR-530313 (R. D. Hume)
Attn: AIR-53051A (P. Kicos)
Attn: AIR-53632E (C. Johnson)
Attn: AIR-620B1 (LCDR K. K. Miles)
Attn: AIR-954 (Tech. Library)
Attn: PMA-2692A1 (R. W. Wills)
Attn: PMA-2694 (T. S. Meek)

Naval Surface Weapons Center
Dahlgren Laboratory
Dahlgren, VA 22448
Attn: CK-2301 (J. E. Mitchell)
Attn: CN-61 (J. S. Nerrie)
Attn: DF-52 (W. S. Lenzi)
Attn: Library

Naval Weapons Center
China Lake, CA 93555
Attn: Code 317 (M. H. Keith)
Attn: Code 3181 (C. Padgett) (2 copies)
Attn: Code 3183 (G. Moncsko)
Attn: Code 3183 (C. Driussi)

Naval Weapons Engineering Support Activity
Systems Analysis Dept.
Bldg 210-2 (ESA-19)
Washington Navy Yard
Washington D.C. 20374
Attn: Code ESA-1923 (C. W. Stokes III) (2 copies)

Warner Robins Air Logistics Center
Robins AFB, GA 31098
Attn: WRALC/MMETE (LT W. Shelton)

Armament Systems, Inc.
712-F North Valley Street
Anaheim, CA 92801
Attn: J. Musch

A. T. Kearney and Company, Inc.
100 South Wacker Drive
Chicago, IL 60606
Attn: R. H. Rose

The BDM Corp.
2600 Yale Blvd SE.
Albuquerque, NM 87106
Attn: A. J. Holten

Bell Helicopter Textron
Division of Textron Inc.
P.O. Box 482
Fort Worth, TX 76101
Attn: Security/Dept. 12, J. R. Johnson

The Boeing Aerospace Company
P.O. Box 3999
Seattle, WA 98124
Attn: J. G. Avery, M/S 4C-08

The Boeing Company
Vertol Division
Boeing Center
P.O. Box 16858
Philadelphia, PA 19142
Attn: J. E. Gonsalves, M/S P32-19 (2 copies)

The Boeing Company
Wichita Division
3801 S. Oliver St.
Wichita, KS 67210
Attn: H. E. Corner, M/S K16-67
Attn: L. D. Lee, M/S K31-11

Calspan Corp.
P.O. Box 235
Buffalo, NY 14221
Attn: Library (V. M. Young)

Cessna Aircraft Co.
Wallace Division
P.O. Box 7704
Wichita, KS 67277
Attn: Engineering Library

COMARCO inc
1417 N. Norma
Ridgecrest, CA 93555
Attn: D. Smith (2 copies)

Falcon Research and Development Co.
2350 Alamo Ave., SE
Albuquerque, NM 87106
Attn: W. L. Baker

Falcon Research and Development Co.
696 Fairmount Ave.
Baltimore, MD 21204
Attn: J. A. Silva

General Dynamics Corp.
Fort Worth Division
Grants Lane, P.O. Box 748
Fort Worth, TX 76101
Attn: P. R. deTonnancour/G. W. Bowen

General Electric Co.
Aircraft Engine Business Group
Evendale Plant
Cincinnati, OH 45215
Attn: AEG Technical Information Center (J. J. Brady)

Goodyear Aerospace Corp.
1210 Massillon Rd.
Akron, OH 44315
Attn: J. E. Wells, D/959G
Attn: Library, D/152G (R. L. Vittitoe/J. R. Wolfersberger) (3 copies)

Grumman Aerospace Corp.
South Oyster Bay Rd.
Bethpage, NY 11714
Attn: J. P. Archey Jr., Dept. 662, Mail C42-05
Attn: R. W. Harvey, Mail C27-05
Attn: H. L. Henze, B16-25
Attn: Technical Information Center, Plant 35 L01-35 (H. B. Smith)

IIT Research Institute
10 West 35 Street
Chicago, IL 60616
Attn: I. Pincus

Lockheed-California Co.
A Division of Lockheed Aircraft Corp.
2555 Hollywood Way
P.O. Box 551
Burbank, CA 91520
Attn: Technological Information Center, 84-40 Unit 35, Plant A-1
Attn: G. E. Raymer, D/75-84 Bldg. 63 A-1 (2 copies)

Lockheed-Georgia Co.
A Division of Lockheed Aircraft Corp.
86 S. Cobb Drive
Marietta, GA 30063
Attn: D. R. Scarbrough, 72-08 Zone 12
Attn: Sci-Tech Info Center, 72-34 Zone 26 (T. J. Kopkin)

Martin Marietta Corp.
Orlando Division
P.O. Box 5837
Orlando, FL 32855
Attn: Library (M. C. Griffith, MP-30)

McDonnell Douglas Corp.
Douglas Aircraft Company
3855 Lakewood Blvd.
Long Beach, CA 90846
Attn: Technical Library, C1-250/36-84 AUTO 14-78 (3 copies)

McDonnell Douglas Corp.
P.O. Box 516
St. Louis, MO 63166
Attn: R. D. Detrich, Dept. 022

Northrop Corp.
Aircraft Division
3901 W. Broadway
Hawthorne, CA 90250
Attn: J. H. Bach, 2130/83
Attn: H. W. Jones, 3360/82

Northrop Corp.
Ventura Division
1515 Rancho Conejo Blvd.
P.O. Box 2500
Newbury Park, CA 91320
Attn: M. Raine

Rockwell International Corp.
Los Angeles Division
5701 W. Imperial Hwy
Los Angeles, CA 90009
Attn: W. L. Jackson
Attn: R. Moonan, AB78 (2 copies)

Southwest Research Institute
P.O. Drawer 28510
San Antonio, TX 78284
Attn: E. D. Esparza (10 copies)
Attn: P. H. Zabel, Div. 02

ABSTRACT CARD

Air Force Flight Dynamics Laboratory

Development of a Blast Simulator for Testing Simulated Aircraft Fuel Tanks, by E. D. Esparza and A. B. Wenzel, Southwest Research Institute, San Antonio, TX. Wright-Patterson AFB, OH, AFFDL, for Joint Technical Coordinating Group/Aircraft Survivability, July 1978. 42 pp. (JTCG/AS-76-T-004, publication UNCLASSIFIED.)

Anti-aircraft missile warheads pose a severe threat to aircraft even when the missile misses the aircraft. The threat from missile warheads can be divided into two primary areas for proximity detonation, fragments and blast. This report describes the development, calibration, and testing of a blast simulator capable of

(Over)

Card UNCLASSIFIED

1 card, 8 copies

Air Force Flight Dynamics Laboratory

Development of a Blast Simulator for Testing Simulated Aircraft Fuel Tanks, by E. D. Esparza and A. B. Wenzel, Southwest Research Institute, San Antonio, TX. Wright-Patterson AFB, OH, AFFDL, for Joint Technical Coordinating Group/Aircraft Survivability, July 1978. 42 pp. (JTCG/AS-76-T-004, publication UNCLASSIFIED.)

Anti-aircraft missile warheads pose a severe threat to aircraft even when the missile misses the aircraft. The threat from missile warheads can be divided into two primary areas for proximity detonation, fragments and blast. This report describes the development, calibration, and testing of a blast simulator capable of

(Over)

Card UNCLASSIFIED

1 card, 8 copies

Air Force Flight Dynamics Laboratory

Development of a Blast Simulator for Testing Simulated Aircraft Fuel Tanks, by E. D. Esparza and A. B. Wenzel, Southwest Research Institute, San Antonio, TX. Wright-Patterson AFB, OH, AFFDL, for Joint Technical Coordinating Group/Aircraft Survivability, July 1978. 42 pp. (JTCG/AS-76-T-004, publication UNCLASSIFIED.)

Anti-aircraft missile warheads pose a severe threat to aircraft even when the missile misses the aircraft. The threat from missile warheads can be divided into two primary areas for proximity detonation, fragments and blast. This report describes the development, calibration, and testing of a blast simulator capable of

(Over)

Card UNCLASSIFIED

1 card, 8 copies

Air Force Flight Dynamics Laboratory

Development of a Blast Simulator for Testing Simulated Aircraft Fuel Tanks, by E. D. Esparza and A. B. Wenzel, Southwest Research Institute, San Antonio, TX. Wright-Patterson AFB, OH, AFFDL, for Joint Technical Coordinating Group/Aircraft Survivability, July 1978. 42 pp. (JTCG/AS-76-T-004, publication UNCLASSIFIED.)

Anti-aircraft missile warheads pose a severe threat to aircraft even when the missile misses the aircraft. The threat from missile warheads can be divided into two primary areas for proximity detonation, fragments and blast. This report describes the development, calibration, and testing of a blast simulator capable of

(Over)

Card UNCLASSIFIED

1 card, 8 copies

JTCG/AS-76-T-004

varying the blast parameters (i.e., pressure, impulse, and time duration), simulating those obtained at various standoff distances from a prototype warhead detonation.

JTCG/AS-76-T-004

varying the blast parameters (i.e., pressure, impulse, and time duration), simulating those obtained at various standoff distances from a prototype warhead detonation.

JTCG/AS-76-T-004

varying the blast parameters (i.e., pressure, impulse, and time duration), simulating those obtained at various standoff distances from a prototype warhead detonation.

JTCG/AS-76-T-004

varying the blast parameters (i.e., pressure, impulse, and time duration), simulating those obtained at various standoff distances from a prototype warhead detonation.

ABSTRACT CARD

Air Force Flight Dynamics Laboratory

Development of a Blast Simulator for Testing Simulated Aircraft Fuel Tanks, by E. D. Esparza and A. B. Wenzel, Southwest Research Institute, San Antonio, TX. Wright-Patterson AFB, OH, AFFDL, for Joint Technical Coordinating Group/Aircraft Survivability, July 1978. 42 pp. (JTCG/AS-76-T-004, publication UNCLASSIFIED.)

Anti-aircraft missile warheads pose a severe threat to aircraft even when the missile misses the aircraft. The threat from missile warheads can be divided into two primary areas for proximity detonation, fragments and blast. This report describes the development, calibration, and testing of a blast simulator capable of

Card UNCLASSIFIED

(Over)
1 card, 8 copies

Air Force Flight Dynamics Laboratory

Development of a Blast Simulator for Testing Simulated Aircraft Fuel Tanks, by E. D. Esparza and A. B. Wenzel, Southwest Research Institute, San Antonio, TX. Wright-Patterson AFB, OH, AFFDL, for Joint Technical Coordinating Group/Aircraft Survivability, July 1978. 42 pp. (JTCG/AS-76-T-004, publication UNCLASSIFIED.)

Anti-aircraft missile warheads pose a severe threat to aircraft even when the missile misses the aircraft. The threat from missile warheads can be divided into two primary areas for proximity detonation, fragments and blast. This report describes the development, calibration, and testing of a blast simulator capable of

Card UNCLASSIFIED

(Over)
1 card, 8 copies

Air Force Flight Dynamics Laboratory

Development of a Blast Simulator for Testing Simulated Aircraft Fuel Tanks, by E. D. Esparza and A. B. Wenzel, Southwest Research Institute, San Antonio, TX. Wright-Patterson AFB, OH, AFFDL, for Joint Technical Coordinating Group/Aircraft Survivability, July 1978. 42 pp. (JTCG/AS-76-T-004, publication UNCLASSIFIED.)

Anti-aircraft missile warheads pose a severe threat to aircraft even when the missile misses the aircraft. The threat from missile warheads can be divided into two primary areas for proximity detonation, fragments and blast. This report describes the development, calibration, and testing of a blast simulator capable of

Card UNCLASSIFIED

(Over)
1 card, 8 copies

Air Force Flight Dynamics Laboratory

Development of a Blast Simulator for Testing Simulated Aircraft Fuel Tanks, by E. D. Esparza and A. B. Wenzel, Southwest Research Institute, San Antonio, TX. Wright-Patterson AFB, OH, AFFDL, for Joint Technical Coordinating Group/Aircraft Survivability, July 1978. 42 pp. (JTCG/AS-76-T-004, publication UNCLASSIFIED.)

Anti-aircraft missile warheads pose a severe threat to aircraft even when the missile misses the aircraft. The threat from missile warheads can be divided into two primary areas for proximity detonation, fragments and blast. This report describes the development, calibration, and testing of a blast simulator capable of

Card UNCLASSIFIED

(Over)
1 card, 8 copies

JTCG/AS-76-T-004

varying the blast parameters (i.e., pressure, impulse, and time duration), simulating those obtained at various standoff distances from a prototype warhead detonation.

JTCG/AS-76-T-004

varying the blast parameters (i.e., pressure, impulse, and time duration), simulating those obtained at various standoff distances from a prototype warhead detonation.

JTCG/AS-76-T-004

varying the blast parameters (i.e., pressure, impulse, and time duration), simulating those obtained at various standoff distances from a prototype warhead detonation.

JTCG/AS-76-T-004

varying the blast parameters (i.e., pressure, impulse, and time duration), simulating those obtained at various standoff distances from a prototype warhead detonation.

Teledyne Ryan Aeronautical
2701 Harbor Dr.
San Diego, CA 92112
Attn: Technical Information Services (W. E. Ebner)

United Technologies Corp.
United Technologies Research Center
Silver Lane, Post 10
East Hartford, CT 06108
Attn: UTC Library (M. E. Donnelly)

United Technologies Corporation
Pratt & Whitney Aircraft Group
Government Products Division
P.O. Box 2691
West Palm Beach, FL 33402
Attn: J. Fyfe, Mail E-39

Vought Corporation
P.O. Box 5907
Dallas, TX 75222
Attn: G. Gilder, 2-51700
Attn: D. M. Reedy, 2-30100